

B. Yang · W. Q. Chen · H. J. Ding

Equilibrium of transversely isotropic FGM plates with an elliptical hole: 3D elasticity solutions

Received: 20 June 2015 / Accepted: 22 February 2016 / Published online: 8 March 2016
© Springer-Verlag Berlin Heidelberg 2016

Abstract A transversely isotropic plate of functionally graded material (FGM) with an elliptical hole subjected to non-lateral loads is analyzed by employing England–Spencer plate theory. The problem is analytically solved by determining the four analytic functions in the general solution to the governing equations when there are no transverse forces acting on the plate surfaces. Three kinds of basic problems are classified according to the boundary conditions. For the first kind problem, which is studied in detail in the paper, the boundary conditions expressed by four real functions are rewritten as two complex function equations. The problem is eventually transformed to a complex function theory problem. Three-dimensional elasticity solutions are obtained for a transversely isotropic FGM plate containing an elliptical hole subject to loads at infinity or on the hole boundary. The conformal mapping technology is used along with the Cauchy integral method. Explicit expressions for the concentration factors of resultant forces are also presented. The present elasticity solutions are exactly the same as those available in the literature if the FGM degenerates to the homogeneous material. When the elliptical hole becomes a circular one, the present elasticity solutions are also found consistent with those obtained in the authors' previous work.

Keywords Functionally graded plates · Transversely isotropic · Elliptical holes · Conformal mapping · Cauchy integrals · Elasticity solutions

B. Yang (✉)
Department of Civil Engineering, Zhejiang Sci-Tech University, Hangzhou 310018, People's Republic of China
E-mail: bo.young@163.com

W. Q. Chen
State Key Lab of CAD & CG, Zhejiang University, Zijingang Campus, Hangzhou 310058, People's Republic of China

W. Q. Chen
Department of Engineering Mechanics, Zhejiang University, Yuquan Campus, Hangzhou 310027, People's Republic of China

W. Q. Chen
Key Laboratory of Soft Machines and Smart Devices of Zhejiang Province, Zhejiang University, Hangzhou 310027, People's Republic of China

H. J. Ding
Department of Civil Engineering, Zhejiang University, Zijingang Campus, Hangzhou 310058, People's Republic of China

List of symbols

x, y, z	Rectangular coordinates
ρ, θ	Polar coordinates
n, t	Curvilinear coordinates with directions normal to and along the boundary
ζ	$x + iy$
η	$\rho e^{i\theta}$
σ	$e^{i\theta}$
L	Boundary of the mid-plane of plate
s	Arc length measured from a certain point on L in a specified direction
S	Region of the mid-plane of plate
γ	Unit circle
a, b	Semi-major and semi-minor axes of the ellipse
R, m	Real constants related to a and b
h	Thickness of plate
$\omega(\eta)$	Mapping function
$\bar{u}, \bar{v}, \bar{w}$	Mid-plane displacements in rectangular coordinates
u, v, w	Displacements in rectangular coordinates
$R_0, \dots, R_4, T_1, \dots, T_4$	Functions of z
$a_1, a_2, a_5, a_6, a_7, b_1, b_2, b_5, b_6, b_7, b_8$	Real constants
$\kappa_1, \dots, \kappa_9$	Real constants
C, B, B_1	Complex constants
$\sigma_x, \sigma_y, \tau_{xy}$	Stress components in rectangular coordinates
$\sigma_n, \sigma_t, \tau_{nt}$	Stress components in curvilinear coordinates
N_x, N_y, N_{xy}	Resultant forces per unit length in rectangular coordinates
M_x, M_y, M_{xy}	Bending and twisting moments per unit length in rectangular coordinates
Q_{xz}, Q_{yz}	Shear forces per unit length in rectangular coordinates
N_n, N_t, N_{nt}	Resultant forces per unit length in curvilinear coordinates
M_n, M_t, M_{nt}	Bending and twisting moments per unit length in curvilinear coordinates
Q_n	Shear force per unit length in curvilinear coordinates
$N_n^b, N_{nt}^b, M_n^b, M_{nt}^b, Q_n^b$	Known functions on the boundary L
p	Known function on the boundary L , corresponding to the effective shear force
X_n, Y_n, Z_n	Stresses acting at the point (x, y, z) on the cylindrical surface perpendicular to the mid-plane of the plate
$N_{xn}, N_{yn}, M_{xn}, M_{yn}$	Resultant forces and moments of X_n, Y_n, Z_n along the thickness of the plate
X, Y, Z, M_X, M_Y	Components of the principal vectors and moments about the origin of external stresses applied on hole boundaries in rectangular coordinates
$\alpha(\zeta), \beta(\zeta), \phi(\zeta), \psi(\zeta)$	Analytical functions of ζ
$A(\zeta)$	The first derivative of $\alpha(\zeta)$
$\beta(\eta), \phi(\eta), \psi(\eta), A(\eta)$	Analytical functions of η
$\{Q\} = \{f_1 + if_2, f_3 + if_4\}^T$	Functions of loads on the boundary
$N_1, N_2, N_{12}, M_1, M_2, M_{12}$	Loads applied at infinity in curvilinear coordinates
$N_n^b, N_{nt}^b, M_n^b, M_{nt}^b$	Loads applied on the boundary of the elliptical hole
K_{ij}	Resultant force concentration factors (RFCFs)
c_{ij}	Material parameters
c_{ij}^0	Material parameters at $z = -h/2$
λ	Gradient index of FGMs

1 Introduction

Homogeneous elastic plates perforated by various holes have widely been used in engineering fields (such as in the design of advanced machinery, pressure vessels, aerospace structures). Their static and dynamic behaviors have been investigated efficiently by different methods, among which the complex variable method is typical. It has been developed and adopted for plane problems in elasticity due to their effectiveness in solving boundary value problems. A series of analytical results for plates with holes have been obtained by the complex variable method as illustrated in the classic books by Muskhelishvili [1], Savin [2] and Lekhnitskii [3]. Recently, using the Schwarz's alternating method and the Muskhelishvili's complex variable method, Zhang et al. [4] derived an efficient and accurate stress solution for an infinite elastic plate around two elliptic holes, subjected to uniform loads on the hole boundaries and at infinity. Pan et al. [5] studied the stress distribution around a rectangular hole in a finite plate under uniaxial tension by using the Muskhelishvili's complex variable method together with the proposed stress functions. Using Muskhelishvili's complex variable method and the conformal mapping technique, Sharma [6] determined analytically the moment distribution around polygonal holes in an infinite isotropic plate subjected to bending/twisting moment at infinity.

As a new type of composite materials, functionally graded materials (FGMs) can be designed artificially and neatly in which the volume fractions of different constituent materials vary continuously from one side to the other, hence leading to no significant internal interface in them. There are a few papers dealing with FGM plates with holes, but most of them considered only two-dimensional (2D) problems and assumed the material is graded along the in-plane radial direction. For instance, Zhang et al. [7] obtained an exact thermoelastic solution for an infinite functionally graded plate with a circular hole when the temperature field varies arbitrarily in the radial direction. Kubair and Bhanu-Chandar [8] investigated the stress concentration around a circular hole in FGM panels under uniaxial tension via an isoparametric finite element formulation. Kubair [9] obtained closed-form expressions for the stresses and displacements in infinite FGM plates without and with holes subjected to anti-plane shear loading. Stress distributions in infinite and finite FGM plates with a circular hole under arbitrary in-plane uniform loads were studied by Yang et al. [10,11], respectively, using the complex variable method combined with the least squares boundary collocation technique. Mohammadi et al. [12] obtained analytical solutions for stress concentration around a circular hole in an infinite FGM plate subjected to uniform biaxial tension and pure shear loading. There are relatively much few studies on three-dimensional (3D) problems of FGM plates with the material properties varying along the thickness direction. Based on the 3D elasticity theory and using a graded boundary element method, Ashrafi et al. [13] presented a static analysis of FGM plates with circular holes subjected to biaxial tensions; they assumed that the material properties vary through the thickness or longitudinal direction in an exponential way.

Based on the 3D theory of elasticity, Spencer and his coauthors (see, for example, Mian and Spencer [14]) have developed a procedure for deriving exact solutions for isotropic FGM plates with tractions-free surfaces by formulating and solving a much simpler 2D plate problem. The material properties can vary arbitrarily with the thickness coordinate. Yang et al. [15] extended the work of Mian and Spencer [14] to a transversely isotropic FGM rectangular plate with opposite edges simply supported and subjected to a uniform load acting on the top and bottom surfaces. Using the complex function theory, England and Spencer [16] reformulated the plate theory in Mian and Spencer [14] in terms of four analytical functions. Hereinafter, this complex formulation will be referred to as England–Spencer plate theory. England [17] further investigated the elastic field in an FGM plate containing a cylindrical hole or a line crack through its thickness under a uniform force field at infinity. England [18] generalized the above plate theory to the case involving the effect of top-surface pressure, which satisfies the biharmonic equation or the higher-order ones. Yang et al. [19,20] extended the England–Spencer plate theory to transversely isotropic FGM plates and obtained a series of 3D elasticity solutions for FGM rectangular and annular plates. Recently, by using Laurent's theorem to express each complex potential as a power series, Yang et al. [21] studied the resultant force concentration in an infinite plate with a circular hole subject to loads at infinity as well as the elastic field in an infinite plate subject to concentrated loads and moments at the origin.

To the best of the authors' knowledge, the 3D problem of FGM plates with elliptical hole has not been addressed. The purpose of this paper is to investigate the 3D equilibrium of a transversely isotropic FGM plate containing an elliptical hole subject to loads applied on the cylindrical boundaries of the plate by using Cauchy integrals. The analysis is based on England–Spencer plate theory and is a further extension of the authors' previous work (Yang et al. [19–21]). The outline of the paper is as follows: The main formulas obtained in our previous papers (Yang et al. [19–21]) are summarized in Sect. 2. According to the boundary conditions on the hole edge, three basic kinds of boundary value problems are classified in Sect. 3. As an example, Sect. 4 shows

how to convert the first kind problem into a complex function theory problem. Based on the Cauchy integral method and the conformal mapping technology, a mathematical procedure is developed to study the problems of an infinite plate with an elliptical hole in Sect. 5. 3D elasticity solutions for such a plate subject to external loads at infinity and on the edge of the hole are presented in Sects. 6 and 7, respectively. The validity and accuracy of the derived solutions are checked by comparing with the ones available in the literature. Section 8 presents some numerical results, and Sect. 9 summarizes the work of the paper.

2 England–Spencer plate theory

A transversely isotropic FGM plate, bounded by the planes $z = \pm h/2$, with the z -axis of the Cartesian coordinates vertically upward, is considered here. The xy plane is the isotropic plane of the material which coincides with the mid-plane of the plate. If the plate is only subject to normal biharmonic pressure $p(x, y)$ on the upper surface, we have $\sigma_z = -p(x, y)$, $\sigma_{xz} = \sigma_{yz} = 0$ at $z = h/2$ and $\sigma_z = \sigma_{xz} = \sigma_{yz} = 0$ at $z = -h/2$.

According to the England–Spencer plate theory (England and Spencer [16]; England [18]), we seek the displacement field in the following form:

$$\begin{aligned} u + iv &= \bar{u} + i\bar{v} + 2\frac{\partial}{\partial\bar{\zeta}} (R_1\Delta + R_0\bar{w} + R_2\nabla^2\bar{w} + R_3\nabla^4\bar{w} + R_4\nabla^6\bar{w}), \\ w &= \bar{w} + T_1\Delta + T_2\nabla^2\bar{w} + T_3\nabla^4\bar{w} + T_4\nabla^6\bar{w}, \end{aligned} \quad (2.1)$$

where $\bar{u} = \bar{u}(x, y)$, $\bar{v} = \bar{v}(x, y)$, and $\bar{w} = \bar{w}(x, y)$ are the mid-plane displacements, $R_0, \dots, R_4, T_1, \dots, T_4$ are functions of z , and

$$\begin{aligned} \Delta &= \bar{u}_{,x} + \bar{v}_{,y}, \quad \nabla^2 = \frac{\partial^2}{\partial x^2} + \frac{\partial^2}{\partial y^2}, \quad \zeta = x + iy, \quad \bar{\zeta} = x - iy, \\ 2\frac{\partial}{\partial\bar{\zeta}} &= \frac{\partial}{\partial x} - i\frac{\partial}{\partial y}, \quad 2\frac{\partial}{\partial\zeta} = \frac{\partial}{\partial x} + i\frac{\partial}{\partial y}, \end{aligned} \quad (2.2)$$

Yang et al. [19] showed that the expressions of functions R_j ($j = 0, \dots, 4$) and T_k ($k = 1, \dots, 4$) and the following governing equations could be obtained by making use of the stress boundary conditions on the upper and lower surfaces of the plate:

$$\frac{\partial}{\partial\bar{\zeta}} [\kappa_1\Delta + \kappa_2\nabla^2\bar{w} + \kappa_3\nabla^4\bar{w} + \kappa_4\nabla^6\bar{w} + i\Omega(x, y)] = 0, \quad (2.3)$$

$$S_1(h/2)\nabla^4\bar{w} = -p(x, y) + S_{21}\nabla^2p(x, y), \quad (2.4)$$

where $\Omega(x, y) = \bar{v}_{,x} - \bar{u}_{,y}$, and the expressions of constants $\kappa_1, \kappa_2, \kappa_3, \kappa_4, S_{21}$ and $S_1(h/2)$ can be found from Appendix of Yang et al. [19].

When $p(x, y) = 0$, Eq. (2.4) gives rise to $\nabla^4\bar{w} = 0$, and hence Eq. (2.1) becomes:

$$\begin{aligned} u + iv &= \bar{u} + i\bar{v} + 2\frac{\partial}{\partial\bar{\zeta}} (R_1\Delta + R_0\bar{w} + R_2\nabla^2\bar{w}), \\ w &= \bar{w} + T_1\Delta + T_2\nabla^2\bar{w}, \end{aligned} \quad (2.5)$$

which was obtained in Yang et al. [15]. It becomes identical with that obtained by Mian and Spencer [14] if the material degenerates from transverse isotropy to isotropy. With Eq. (2.5), the expressions of the mid-plane displacements and resultant forces may be expressed in terms of four analytical functions ($\alpha(\zeta)$, $\beta(\zeta)$, $\phi(\zeta)$ and $\psi(\zeta)$) as follows:

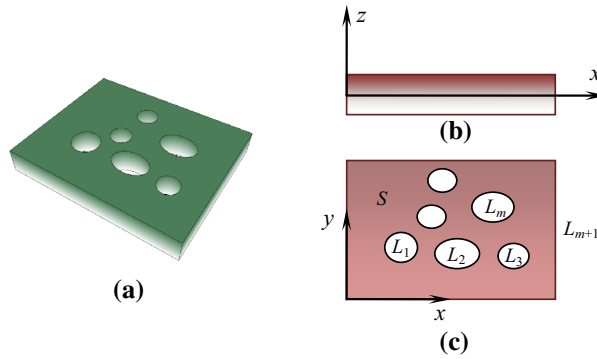


Fig. 1 FGM plate with holes and the coordinates: **a** 3D view, **b** front view, and **c** top view

$$\bar{w} = \alpha(\zeta) + \overline{\alpha(\zeta)} + \bar{\zeta}\beta(\zeta) + \zeta\overline{\beta(\zeta)}, \tag{2.6}$$

$$D = \bar{u} + i\bar{v} = \frac{\kappa_1 + 1}{\kappa_1 - 1}\phi(\zeta) - \zeta\overline{\phi'(\zeta)} - \overline{\psi(\zeta)} - 2\frac{\kappa_2}{\kappa_1}[\beta(\zeta) + \zeta\overline{\beta'(\zeta)}], \tag{2.7}$$

$$N_x + N_y = a_1[\phi'(\zeta) + \overline{\phi'(\zeta)}] + 4a_2[\beta'(\zeta) + \overline{\beta'(\zeta)}], \tag{2.8}$$

$$N_y - N_x + 2iN_{xy} = a_1[\bar{\zeta}\phi''(\zeta) + \psi'(\zeta)] - a_5\phi'''(\zeta) + 4a_2\bar{\zeta}\beta''(\zeta) + 2a_6\alpha''(\zeta) - a_7\beta'''(\zeta), \tag{2.9}$$

$$M_x + M_y = -b_1[\phi'(\zeta) + \overline{\phi'(\zeta)}] + 4b_2[\beta'(\zeta) + \overline{\beta'(\zeta)}], \tag{2.10}$$

$$M_y - M_x + 2iM_{xy} = a_6[\bar{\zeta}\phi''(\zeta) + \psi'(\zeta)] - b_5\phi'''(\zeta) + b_6\bar{\zeta}\beta''(\zeta) + b_7\alpha''(\zeta) - b_8\beta'''(\zeta), \tag{2.11}$$

$$Q_{xz} - iQ_{yz} = -(b_1 + a_6)\phi''(\zeta) + (4b_2 - b_6)\beta''(\zeta), \tag{2.12}$$

where $a_1, a_2, a_5, a_6, a_7, b_1, b_2, b_5, b_6, b_7, b_8$ are real constants (see [19]) and the prime represents derivative with respect to ζ . Equations (2.6)–(2.12) are the general solution to the corresponding homogeneous equations of Eqs. (2.3) and (2.4). It can be used to solve various problems of FGM plates subject to loads applied on the cylindrical boundary.

3 Boundary conditions and basic problems

In England–Spencer plate theory, there are only four analytical functions in the general solution and they fully determine the mid-plane displacements of the plate. Therefore, it is impossible for the three-dimensional exact solutions which are derived based on these analytical functions to meet the cylindrical boundary conditions of the plate point by point. However, we can in an approximate sense allow the three-dimensional solutions just to meet four specified boundary conditions on the boundary L of the region S in the plate. The region S can be either simply connected or multiply connected, and accordingly the boundary L can be either a single smooth contour or a collection of contours $L_1, L_2, \dots, L_m, L_{m+1}$ (for a finite region) or a collection of contours L_1, L_2, \dots, L_m (for an infinite region). As a result, the original boundary value problem in three-dimensional elasticity is transformed into a 2D one which just concerns the deformation of the mid-plane of the plate. An FGM plate with holes is shown in Fig. 1 along with the coordinates. Suppose that the mid-plane displacements and resultant forces of the plate are all continuous in the region S and to the boundary L . The following three kinds of boundary conditions are considered from the viewpoint of mechanics:

(1) Free boundary conditions

$$N_n(t) = N_n^b(s), \quad N_{nt}(t) = N_{nt}^b(s), \quad M_n(t) = M_n^b(s), \quad Q_n(t) + \frac{\partial M_{nt}(t)}{\partial s} = p(s), \tag{3.1}$$

where $N_n^b(s), N_{nt}^b(s), M_n^b(s), M_{nt}^b(s), Q_n^b(s)$, and $p(s) = Q_n^b(s) + \frac{\partial M_{nt}^b(s)}{\partial s}$ are known functions on the boundary L , corresponding to the normal force, tangential force, moment, torque, shear force and the effective

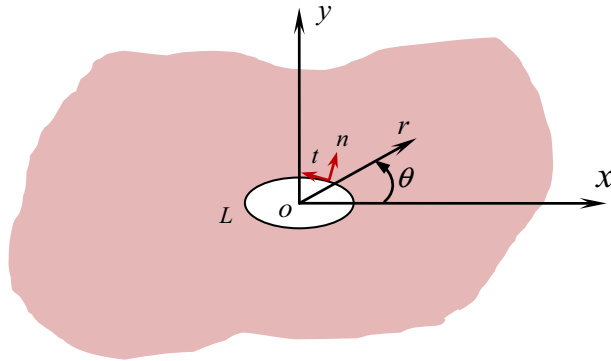


Fig. 2 Mid-plane of an infinite FGM plate containing a hole

shear force, respectively; s is the arc length measured from a certain point on L in a specified direction; subscripts n and t represent the outward normal and tangential direction of L (see Fig. 2 for an infinite plate with a hole), respectively; and $t = x(s) + iy(s)$ is a point on L with $x(s)$ and $y(s)$ being the coordinates of the boundary point. Obviously, there is a one-to-one mapping between t and s .

(2) Clamped boundary conditions

$$\bar{u}(t) = \bar{u}^b(s), \quad \bar{v}(t) = \bar{v}^b(s), \quad \bar{w}(t) = \bar{w}^b(s), \quad \frac{\partial \bar{w}(t)}{\partial n} = W_n(s), \quad (3.2)$$

where $\bar{u}^b(s)$, $\bar{v}^b(s)$, $\bar{w}^b(s)$ and $W_n(s)$ are known functions on the boundary L .

(3) Simply supported boundary conditions

$$N_n(t) = N_n^b(s), \quad M_n(t) = M_n^b(s), \quad \bar{w}(t) = \bar{w}^b(s), \quad \bar{u}_t(t) = \bar{u}_t^b(s), \quad (3.3)$$

where $\bar{u}_t(t)$ is the displacement component in the tangential direction of the point on L and $\bar{u}_t^b(s)$ is the known function.

The boundary value problem of a plate with the free boundary conditions on the boundary L is classified as the first kind basic problem, while that of a plate with clamped or simply supported boundary conditions on L is classified as the second or third kind basic problem. In addition, there can be mixed types of boundary conditions on L . In fact, many interesting and important problems have mixed boundary conditions, such as the problem of a rectangular plate with two opposite edges simply supported and the problem of a cantilever rectangular plate.

By virtue of Eqs. (2.6)–(2.12), the terms in the left-hand sides of Eqs. (3.1)–(3.3) can be expressed by the boundary values of the four analytical functions $\alpha(\zeta)$, $\beta(\zeta)$, $\phi(\zeta)$, $\psi(\zeta)$ and their derivatives. Eventually, the four analytical functions can be determined from the boundary conditions. To proceed, the following transform for the displacement and stress components between coordinates (n, t) and coordinates (x, y) shall be adopted:

$$\bar{u}_n + i\bar{u}_t = (\bar{u} + i\bar{v})e^{-i\mathcal{U}}, \quad (3.4)$$

$$\sigma_n + \sigma_t = \sigma_x + \sigma_y, \quad \sigma_t - \sigma_n + 2i\tau_{nt} = (\sigma_y - \sigma_x + 2i\tau_{xy})e^{2\mathcal{U}i}, \quad (3.5)$$

$$N_n + N_t = N_x + N_y, \quad N_t - N_n + 2iN_{nt} = (N_y - N_x + 2iN_{xy})e^{2\mathcal{U}i}, \quad (3.6)$$

$$M_n + M_t = M_x + M_y, \quad M_t - M_n + 2iM_{nt} = (M_y - M_x + 2iM_{xy})e^{2\mathcal{U}i}, \quad (3.7)$$

where \mathcal{U} is the angle between the axes n and x , and

$$(N_n, N_t, N_{nt}, M_n, M_t, M_{nt}) = \int_{-\frac{h}{2}}^{\frac{h}{2}} (\sigma_n, \sigma_t, \tau_{nt}, \sigma_n z, \sigma_t z, \tau_{nt} z) dz. \quad (3.8)$$

4 The first kind basic problem

The mid-plane displacements and resultant forces are expressed in terms of the four analytical functions. If the boundary conditions can be rewritten as two complex function equations by an appropriate combination, we

will lead to a complex function theory problem. That is, we are facing with the task to determine the expressions of the four analytical functions in the region S when the values of the two function equations consisting of the four analytical functions and their derivatives are known on the boundary L . In the process of transforming Eq. (3.1), (3.2) or (3.3) to two complex function equations, it will facilitate solving these two equations if we can perform integration along L so as to reduce the order of derivatives of the complex functions in the boundary conditions. In the following, the first kind basic problem will be addressed in detail for illustration.

Firstly, integrating Eq. (3.1)₄ along L leads to

$$Q + M_{nt} = P(s) + e_0, \tag{4.1}$$

where e_0 is a real integral constant, and

$$Q(t) = \int Q_n ds, \quad P(s) = \int p(s) ds = \int Q_n^b(s) ds + M_{nt}^b(s). \tag{4.2}$$

Combining Eqs. (3.1)₁ with (3.1)₂ and Eqs. (3.1)₃ with (4.1), respectively, we obtain the following complex forms

$$N_n(t) - iN_{nt}(t) = N_n^b(s) - iN_{nt}^b(s). \tag{4.3}$$

$$M_n(t) - iM_{nt}(t) - iQ(t) = M_n^b(s) - iP(s) - ie_0. \tag{4.4}$$

By multiplying Eqs. (4.3) and (4.4) by $e^{-i\Omega}$ and integrating along L , respectively, we find that

$$\int (N_{xn} - iN_{yn}) ds = \int [N_n^b(s) - iN_{nt}^b(s)] e^{-i\Omega} ds, \tag{4.5}$$

$$\int (M_{xn} - iM_{yn} - iQe^{-i\Omega}) ds = \int [M_n^b(s) - iP(s) - ie_0] e^{-i\Omega} ds, \tag{4.6}$$

where the expressions of N_{xn} , N_{yn} , M_{xn} and M_{yn} are shown to be

$$(N_{xn}, N_{yn}, Q_n) = \int_{-\frac{h}{2}}^{\frac{h}{2}} (X_n, Y_n, Z_n) dz, \quad (M_{xn}, M_{yn}) = \int_{-\frac{h}{2}}^{\frac{h}{2}} (X_n, Y_n) z dz, \tag{4.7}$$

in which X_n , Y_n , Z_n are stresses acting at the point (x, y, z) on the cylindrical surface perpendicular to the mid-plane of the plate. They are exerted on the cylindrical surface from the positive side of the normal n . Meanwhile, the following equations have been used

$$N_n - iN_{nt} = (N_{xn} - iN_{yn}) e^{i\Omega}, \quad M_n - iM_{nt} = (M_{xn} - iM_{yn}) e^{i\Omega}. \tag{4.8}$$

We have

$$(N_{xn}, N_{yn}, Q_n, M_{xn}, M_{yn}) = (N_x, N_{xy}, Q_{xz}, M_x, M_{xy}) \cos(n, x) + (N_{xy}, N_y, Q_{yz}, M_{xy}, M_y) \cos(n, y). \tag{4.9}$$

Substituting Eq. (4.9)₃ into Eq. (4.2)₁ and making use of Eq. (2.12), we obtain

$$Q = -\frac{1}{2}i \left\{ -(b_1 + a_6) [\phi'(\zeta) - \overline{\phi'(\zeta)}] + (4b_2 - b_6) [\beta'(\zeta) - \overline{\beta'(\zeta)}] \right\}. \tag{4.10}$$

Substituting Eq. (4.9) into Eqs. (4.5) and (4.6) gives

$$\frac{1}{2} \int [(N_y - N_x + 2iN_{xy}) d\zeta + (N_x + N_y) d\bar{\zeta}] = \int [N_n^b(s) - iN_{nt}^b(s)] d(x - iy). \tag{4.11}$$

$$\frac{1}{2} \int [(M_y - M_x + 2iM_{xy}) d\zeta + (M_x + M_y - 2iQ) d\bar{\zeta}] = \int [M_n^b(s) - iP(s) - ie_0] d(x - iy). \tag{4.12}$$

Substituting Eqs. (2.8) and (2.9) into Eq. (4.11) and Eqs. (2.10), (2.11) and (4.10) into Eq. (4.12) and then integrating gives rise to

$$a_1 [\bar{i}\phi'(t) + \overline{\phi(t)} + \psi(t)] + 4a_2 [\bar{i}\beta'(t) + \overline{\beta(t)}] + 2a_6\alpha'(t) - a_5\phi''(t) - a_7\beta''(t) = \bar{f} = f_1 - if_2 + c_1, \tag{4.13}$$

$$a_6 [\bar{i}\phi'(t) + \psi(t)] + b_6\bar{i}\beta'(t) + b_7\alpha'(t) - b_5\phi''(t) - b_8\beta''(t) - (2b_1 + a_6)\overline{\phi(t)} + (8b_2 - b_6)\overline{\beta(t)} = \bar{F} = f_3 - if_4 + ie_1\bar{i} + c_2, \tag{4.14}$$

where c_1 and c_2 are complex constants, $e_1 = -2e_0$, and

$$f_1 - if_2 = 2 \int [N_n^b(s) - iN_{nt}^b(s)] d(x - iy) = -2i \int [N_{xn}^b(s) - iN_{yn}^b(s)] ds, \tag{4.15}$$

$$f_3 - if_4 = 2 \int [M_n^b(s) - iP(s)] d(x - iy) = -2i \int [M_{xn}^b(s) - iM_{yn}^b(s) - iZ^b(s) e^{-i\zeta}] ds, \tag{4.16}$$

where $N_{xn}^b(s)$, $N_{yn}^b(s)$, $Q_n^b(s)$, $M_{xn}^b(s)$ and $M_{yn}^b(s)$ can be calculated from Eq. (4.7) and

$$Z^b(s) = \int Q_n^b(s) ds. \tag{4.17}$$

By virtue of Eq. (4.8)₁, it can be found that the following equations are equivalent to the boundary conditions (3.1)

$$N_{xn}(t) - iN_{yn}(t) = N_{xn}^b(s) - iN_{yn}^b(s),$$

$$M_n(t) - iM_{nt}(t) - iQ(t) = M_n^b(s) - iP(s) - ie_0. \tag{4.18}$$

Equations (4.13) and (4.14) are the complex forms of the boundary conditions (3.1) or (4.18) which contain three integral constants c_1 , c_2 and e_1 . In a multiply connected region, these three integral constants are generally different along the contours. However, the three constants always can be made zero along a certain contour. For a finite singly connected region, the holomorphic functions $\alpha(\zeta)$, $\beta(\zeta)$, $\phi(\zeta)$ and $\psi(\zeta)$ can be determined from the boundary conditions (4.13) and (4.14) on only one boundary L . The integral constant e_1 in Eq. (4.14) can be taken as zero since β_1^i (the imaginary part of β_1) with the term $i\beta_1^i\zeta$ in the function $\beta(\zeta)$, which doesn't show up in the expressions of the mid-plane displacements and resultant forces of the plate, can be arbitrary. Constants c_1 and c_2 along with constants β_0 and ϕ_0 in functions $\beta(\zeta)$ and $\phi(\zeta)$ simultaneously contribute to the constant terms in Eqs. (4.13) and (4.14). Thus, we can also take $c_1 = 0$ and $c_2 = 0$ because of the arbitrariness of the constants ϕ_0 and β_0 (see Eq. (2.16) in Yang et al. [21]).

For an infinite region S containing a hole, as shown in Fig. 2, L becomes the boundary of the hole and the integral constants can be treated in the same way. It is noted that the four holomorphic functions are usually multi-valued, with the following expressions under the boundedness condition for resultant forces at infinity (see Yang et al. [21])

$$\alpha(\zeta) = \bar{B}\zeta \ln\zeta + A \ln\zeta + \alpha_1\zeta + \alpha_2\zeta^2 + \alpha_0(\zeta), \tag{4.19}$$

$$\beta(\zeta) = B \ln\zeta + \beta_1\zeta + \beta_0(\zeta), \tag{4.20}$$

$$\phi(\zeta) = C \ln\zeta + \phi_1\zeta + \phi_0(\zeta), \tag{4.21}$$

$$\psi(\zeta) = B_1 \ln\zeta + \psi_1\zeta + \psi_0(\zeta), \tag{4.22}$$

where

$$C = \kappa_5(X + iY), \quad B = \kappa_6(M_Y - iM_X) + \kappa_7(X + iY),$$

$$B_1 = \kappa_8(M_Y + iM_X) + \kappa_9(X - iY). \tag{4.23}$$

$$[\alpha_0(\zeta), \beta_0(\zeta), \phi_0(\zeta), \psi_0(\zeta)] = [\alpha_0, \beta_0, \phi_0, \psi_0] + \sum_{n=1}^{\infty} [\alpha_{-n}, \beta_{-n}, \phi_{-n}, \psi_{-n}] \zeta^{-n}. \tag{4.24}$$

It can be shown that α_2 , ϕ_1 (the real part of ϕ_1), β_1^r (the real part of β_1) and ψ_1 are related to the stresses at infinity; ϕ_1^i (the imaginary part of ϕ_1) is proportional to the rigid-body rotation at infinity and hence can be

taken as zero; β_1'' (the imaginary part of β_1) has no relation with the displacements and resultant forces and can be taken as zero; α_1 is related to the rigid-body rotation but nothing with the resultant forces and may be chosen arbitrarily.

Substituting Eqs. (4.19)–(4.22) into Eqs. (4.13) and (4.14) leads to the task to determine the expressions of the four holomorphic functions $\alpha_0(\zeta)$, $\beta_0(\zeta)$, $\phi_0(\zeta)$ and $\psi_0(\zeta)$ in the region S . The corresponding boundary conditions are as follows

$$a_1 [\bar{t}\phi_0'(t) + \overline{\phi_0(t)} + \psi_0(t)] + 4a_2 [\bar{t}\beta_0'(t) + \overline{\beta_0(t)}] + 2a_6\alpha_0'(t) - a_5\phi_0''(t) - a_7\beta_0''(t) = \bar{f}^0 = f_1^0 - if_2^0, \tag{4.25}$$

$$b_7\alpha_0'(t) + (8b_2 - b_6)\overline{\beta_0(t)} - (2b_1 + a_6)\overline{\phi_0(t)} + a_6\psi_0(t) + a_6\bar{t}\phi_0'(t) + b_6\bar{t}\beta_0'(t) - b_5\phi_0''(t) - b_8\beta_0''(t) = \bar{F}^0 = f_3^0 - if_4^0, \tag{4.26}$$

where

$$f_1^0 - if_2^0 = f_1 - if_2 - 2a_6(\bar{B} + \alpha_1) - (a_1\psi_1 + 4a_6\alpha_2)t - [a_1(\phi_1 + \bar{\phi}_1) + 4a_2(\beta_1 + \bar{\beta}_1)]\bar{t} - (a_1C + 4a_2B)\bar{t}t^{-1} - 2a_6At^{-1} - (a_5C + a_7B)t^{-2} - (a_1\bar{C} + 4a_2\bar{B})\ln\bar{t} - \left[a_1 \left(2\frac{\kappa_2}{\kappa_1}\bar{B} - \frac{\kappa_1 + 1}{\kappa_1 - 1}\bar{C} \right) + 2a_6\bar{B} \right] \ln t. \tag{4.27}$$

$$f_3^0 - if_4^0 = f_3 - if_4 - b_7(\bar{B} + \alpha_1) - (a_6\psi_1 + 2b_7\alpha_2)t - [a_6\phi_1 + b_6\beta_1 - (2b_1 + a_6)\bar{\phi}_1 + (8b_2 - b_6)\bar{\beta}_1]\bar{t} - (a_6C + b_6B)\bar{t}t^{-1} - b_7At^{-1} - (b_5C + b_8B)t^{-2} - [(8b_2 - b_6)\bar{B} - (2b_1 + a_6)\bar{C}]\ln\bar{t} - \left[a_6 \left(2\frac{\kappa_2}{\kappa_1}\bar{B} - \frac{\kappa_1 + 1}{\kappa_1 - 1}\bar{C} \right) + b_7\bar{B} \right] \ln t. \tag{4.28}$$

Equations (4.25) and (4.26) show that the right-hand sides should be single-valued functions of t along the contours, which can be proved by using Eqs. (4.27) and (4.28).

In the first kind basic problem, the function $\alpha'(\zeta)$ rather than $\alpha(\zeta)$ appears in the expressions of the resultant forces and boundary conditions. For convenience, the following new function is introduced

$$A(\zeta) = \alpha'(\zeta). \tag{4.29}$$

Equations (4.13) and (4.14) can be rewritten in the following matrix forms

$$[E]\{\overline{\Phi(t)}\} + [F]\bar{t}\{\Phi(t)\}' + [G]\{\Phi(t)\}'' + [H]\{\Psi(t)\} = \{\bar{Q}\}, \tag{4.30}$$

where $\{\bar{Q}\} = \{\bar{f}, \bar{F}\}^T$, $\bar{f} = f_1 - if_2$ and $\bar{F} = f_3 - if_4$, and

$$[E] = \begin{bmatrix} a_1 & 4a_2 \\ -2b_1 - a_6 & 8b_2 - b_6 \end{bmatrix}, \quad [F] = \begin{bmatrix} a_1 & 4a_2 \\ a_6 & b_6 \end{bmatrix}, \quad [G] = \begin{bmatrix} -a_5 & -a_7 \\ -b_5 & -b_8 \end{bmatrix}, \\ [H] = \begin{bmatrix} a_1 & 2a_6 \\ a_6 & b_7 \end{bmatrix}, \quad \{\Phi(t)\} = \begin{Bmatrix} \phi(t) \\ \beta(t) \end{Bmatrix}, \quad \{\Psi(t)\} = \begin{Bmatrix} \psi(t) \\ A(t) \end{Bmatrix}. \tag{4.31}$$

The conjugate expression of Eq. (4.30) is as follows

$$[E]\{\Phi(t)\} + [F]t\{\overline{\Phi(t)}\}' + [G]\{\overline{\Phi(t)}\}'' + [H]\{\overline{\Psi(t)}\} = \{Q\}. \tag{4.32}$$

5 Conformal mapping

Suppose that the two complex variables ζ and η are related by

$$\zeta = \omega(\eta), \tag{5.1}$$

where the function $\omega(\eta)$ is a single-valued analytic function within a certain domain Σ in the complex plane η . Equation (5.1) means that each point η in the domain Σ corresponds to a point ζ within a certain domain S in the plane ζ and that is true vice versa. To ensure that the conformal transformation is mutually one-to-one, $\omega'(\eta)$ cannot be zero in the domain Σ .

If domains Σ and S all are infinite and correspond with each other at infinity, we have

$$\omega(\eta) = R\eta + P(\eta), \tag{5.2}$$

where R is a constant. Function $P(\eta)$ is holomorphic in an infinite domain, which means that it is holomorphic in any finite part of this domain, while it can be expressed in the following series form for sufficiently large $|\zeta|$

$$P(\eta) = a_0 + \sum_{n=1}^{\infty} \frac{a_n}{\eta^n}.$$

As for the transformation which maps the infinite region S surrounded by a simple and closed contour L in the ζ plane into Σ , the exterior of the unit circle γ , in the η plane, we use $\zeta = t$ to represent a point on L and $\eta = \sigma = e^{i\theta}$ a point on γ . Suppose that Eq. (5.1) is continuous to the boundary and hence we have $t = \omega(\sigma)$.

Now let us use $\phi_1(\zeta)$ to represent $\phi(\zeta)$ that was used earlier and introduce the following new notations

$$\phi(\eta) = \phi_1(\zeta) = \phi_1[\omega(\eta)]. \tag{5.3}$$

$$\phi'_1(\zeta) = \frac{d\phi_1(\zeta)}{d\zeta} = \frac{d\phi(\eta)}{d\zeta} = \frac{d\phi(\eta)}{d\eta} \frac{d\eta}{d\zeta} = \phi'(\eta) \frac{1}{\omega'(\eta)}. \tag{5.4}$$

$$\begin{aligned} \phi''_1(\zeta) &= \frac{d}{d\zeta} \left[\phi'(\eta) \frac{1}{\omega'(\eta)} \right] = \left[\phi'(\eta) \frac{1}{\omega'(\eta)} \right]' \frac{1}{\omega'(\eta)} \\ &= \phi''(\eta) \frac{1}{\omega'(\eta)^2} - \phi'(\eta) \frac{\omega''(\eta)}{\omega'(\eta)^3}. \end{aligned} \tag{5.5}$$

Similar formulas can be established for $\alpha_1(\zeta)$, $\beta_1(\zeta)$ and $\psi_1(\zeta)$. For example, we have

$$\alpha(\eta) = \alpha_1(\zeta) = \alpha_1[\omega(\eta)]. \tag{5.6}$$

and

$$A(\eta) = A_1(\zeta) = A_1[\omega(\eta)]. \tag{5.7}$$

By making use of Eqs. (5.3), (5.4), (5.5) and (5.7), we can rewrite Eqs. (4.30) and (4.32) in the following form

$$\begin{aligned} [E] \{ \overline{\Phi(\sigma)} \} + [F] \frac{\overline{\omega(\sigma)}}{\omega'(\sigma)} \{ \Phi(\sigma) \}' + [G] \frac{1}{\omega'(\sigma)^2} \{ \Phi(\sigma) \}'' \\ - [G] \frac{\omega''(\sigma)}{\omega'(\sigma)^3} \{ \Phi(\sigma) \}' + [H] \{ \Psi(\sigma) \} = \{ \bar{Q} \}, \end{aligned} \tag{5.8}$$

$$\begin{aligned} [E] \{ \Phi(\sigma) \} + [F] \frac{\omega(\sigma)}{\omega'(\sigma)} \{ \overline{\Phi(\sigma)} \}' + [G] \frac{1}{\omega'(\sigma)^2} \{ \overline{\Phi(\sigma)} \}'' \\ - [G] \frac{\overline{\omega''(\sigma)}}{\omega'(\sigma)^3} \{ \overline{\Phi(\sigma)} \}' + [H] \{ \overline{\Psi(\sigma)} \} = \{ Q \}, \end{aligned} \tag{5.9}$$

in which $\{Q\}$ is expressed as a function of σ by virtue of $t = \omega(\sigma)$, and

$$\{ \Phi(\sigma) \} = \begin{Bmatrix} \phi(\sigma) \\ \beta(\sigma) \end{Bmatrix}, \quad \{ \Psi(\sigma) \} = \begin{Bmatrix} \psi(\sigma) \\ A(\sigma) \end{Bmatrix}. \tag{5.10}$$

For an infinite region S containing a hole, we may obtain from Eq. (4.19) that

$$A(\zeta) = \alpha'(\zeta) = \bar{B} \ln \zeta + 2\alpha_2 \zeta + A_0(\zeta), \tag{5.11}$$

where

$$A_0(\zeta) = \bar{B} + A\zeta^{-1} + \alpha_1 + \alpha'_0(\zeta) = \bar{B} + \alpha_1 + A\zeta^{-1} - \sum_{n=1}^{\infty} n\alpha_{-n}\zeta^{-n-1} = A_0 + \sum_{n=1}^{\infty} A_{-n}\zeta^{-n}. \tag{5.12}$$

Obviously

$$A_0 = \bar{B} + \alpha_1, \quad A_{-1} = A, \quad A_{-n} = -(n-1)\alpha_{-n+1}, \quad (n = 2, 3, \dots). \tag{5.13}$$

Just as $\beta_0(\zeta)$, $\phi_0(\zeta)$ and $\psi_0(\zeta)$, $A_0(\zeta)$ in Eq. (5.12) is also a holomorphic function in the infinite region. It will be more convenient to use $\beta(\zeta)$, $\phi(\zeta)$, $\psi(\zeta)$ and $A(\zeta)$ in solving the first kind basic problem.

The exterior of an ellipse can be mapped conformally onto that of a circle by

$$\zeta = \omega(\eta) = R \left(\eta + \frac{m}{\eta} \right), \quad R = \frac{a+b}{2} > 0, \quad 0 \leq m = \frac{a-b}{a+b} < 1, \tag{5.14}$$

where a and b are semi-major and minor axes of the ellipse.

By substituting Eq. (5.14) into Eqs. (4.20)–(4.22), (5.11), (4.24) and (5.12), we obtain

$$\beta(\eta) = B \ln \eta + R\beta_1 \eta + \beta_0(\eta), \tag{5.15}$$

$$\phi(\eta) = C \ln \eta + R\phi_1 \eta + \phi_0(\eta), \tag{5.16}$$

$$\psi(\eta) = B_1 \ln \eta + R\psi_1 \eta + \psi_0(\eta), \tag{5.17}$$

$$A(\eta) = \bar{B} \ln \eta + 2\alpha_2 R \eta + A_0(\eta), \tag{5.18}$$

where $\beta_0(\eta)$, $\phi_0(\eta)$, $\psi_0(\eta)$ and $A_0(\eta)$ are all holomorphic in the infinite region.

Equations (5.15)–(5.18) can be rewritten in the following matrix form

$$\{\Phi(\eta)\} = \begin{Bmatrix} \phi(\eta) \\ \beta(\eta) \end{Bmatrix} = \begin{Bmatrix} C \\ B \end{Bmatrix} \ln \eta + R \begin{Bmatrix} \phi_1 \\ \beta_1 \end{Bmatrix} \eta + \{\Phi_0(\eta)\}, \tag{5.19}$$

$$\{\Psi(\eta)\} = \begin{Bmatrix} \psi(\eta) \\ A(\eta) \end{Bmatrix} = \begin{Bmatrix} B_1 \\ \bar{B} \end{Bmatrix} \ln \eta + R \begin{Bmatrix} \psi_1 \\ 2\alpha_2 \end{Bmatrix} \eta + \{\Psi_0(\eta)\}, \tag{5.20}$$

in which

$$\{\Phi_0(\eta)\} = \begin{Bmatrix} \phi_0(\eta) \\ \beta_0(\eta) \end{Bmatrix}, \quad \{\Psi_0(\eta)\} = \begin{Bmatrix} \psi_0(\eta) \\ A_0(\eta) \end{Bmatrix}, \tag{5.21}$$

By substituting the boundary values of functions $\{\Phi(\eta)\}$ and $\{\Psi(\eta)\}$ in Eqs. (5.19) and (5.20) into Eq. (5.8), we have

$$\begin{aligned} & [E] \overline{\{\Phi_0(\sigma)\}} + [F] \frac{\overline{\omega(\sigma)}}{\omega'(\sigma)} \{\Phi_0(\sigma)\}' + [G] \frac{1}{\omega'(\sigma)^2} \{\Phi_0(\sigma)\}'' \\ & - [G] \frac{\omega''(\sigma)}{\omega'(\sigma)^3} \{\Phi_0(\sigma)\}' + [H] \{\Psi_0(\sigma)\} = \{\bar{Q}^0\}, \end{aligned} \tag{5.22}$$

where

$$\begin{aligned} \{\bar{Q}^0\} = & \{\bar{Q}\} + [E] \begin{Bmatrix} \bar{C} \\ \bar{B} \end{Bmatrix} \ln \sigma - R [E] \begin{Bmatrix} \phi_1 \\ \beta_1 \end{Bmatrix} \frac{1}{\sigma} - [F] \begin{Bmatrix} C \\ B \end{Bmatrix} \frac{\overline{\omega(\sigma)}}{\sigma \omega'(\sigma)} \\ & - R [F] \begin{Bmatrix} \phi_1 \\ \beta_1 \end{Bmatrix} \frac{\overline{\omega(\sigma)}}{\omega'(\sigma)} + [G] \begin{Bmatrix} C \\ B \end{Bmatrix} \frac{1}{\sigma^2 \omega'(\sigma)^2} + [G] \begin{Bmatrix} C \\ B \end{Bmatrix} \frac{\omega''(\sigma)}{\sigma \omega'(\sigma)^3} \\ & + R [G] \begin{Bmatrix} \phi_1 \\ \beta_1 \end{Bmatrix} \frac{\omega''(\sigma)}{\omega'(\sigma)^3} - [H] \begin{Bmatrix} B_1 \\ \bar{B} \end{Bmatrix} \ln \sigma - R [H] \begin{Bmatrix} \psi_1 \\ 2\alpha_2 \end{Bmatrix} \sigma. \end{aligned} \tag{5.23}$$

The conjugate formula of Eq. (5.22) is

$$\begin{aligned}
 [E] \{\Phi_0(\sigma)\} + [F] \frac{\omega(\sigma)}{\omega'(\sigma)} \{\overline{\Phi_0(\sigma)}\}' + [G] \frac{1}{\omega'(\sigma)^2} \{\overline{\Phi_0(\sigma)}\}'' \\
 - [G] \frac{\overline{\omega''(\sigma)}}{\omega'(\sigma)^3} \{\overline{\Phi_0(\sigma)}\}' + [H] \{\overline{\Psi_0(\sigma)}\} = \{Q^0\}.
 \end{aligned}
 \tag{5.24}$$

Substituting Eq. (5.14) into Eqs. (5.22)–(5.24) leads to

$$\begin{aligned}
 [E] \{\overline{\Phi_0(\sigma)}\} + [F] \sigma \frac{1+m\sigma^2}{\sigma^2-m} \{\Phi_0(\sigma)\}' + [G] \frac{\sigma^4}{R^2(\sigma^2-m)^2} \{\Phi_0(\sigma)\}'' \\
 - [G] \frac{2m\sigma^3}{R^2(\sigma^2-m)^3} \{\Phi_0(\sigma)\}' + [H] \{\Psi_0(\sigma)\} = \{\overline{Q^0}\}.
 \end{aligned}
 \tag{5.25}$$

$$\begin{aligned}
 \{\overline{Q^0}\} = \{\overline{Q}\} + [E] \left\{ \frac{\overline{C}}{\overline{B}} \right\} \ln \sigma - R [E] \left\{ \frac{\phi_1}{\beta_1} \right\} \frac{1}{\sigma} - [F] \left\{ \frac{C}{B} \right\} \frac{1+m\sigma^2}{\sigma^2-m} \\
 - R [F] \left\{ \frac{\phi_1}{\beta_1} \right\} \sigma \frac{1+m\sigma^2}{\sigma^2-m} + [G] \left\{ \frac{C}{B} \right\} \frac{\sigma^2}{R^2(\sigma^2-m)^2} \\
 + [G] \left\{ \frac{C}{B} \right\} \frac{2m\sigma^2}{R^2(\sigma^2-m)^3} + R [G] \left\{ \frac{\phi_1}{\beta_1} \right\} \frac{2m\sigma^3}{R^2(\sigma^2-m)^3} \\
 - [H] \left\{ \frac{B_1}{\overline{B}} \right\} \ln \sigma - R [H] \left\{ \frac{\psi_1}{2\alpha_2} \right\} \sigma.
 \end{aligned}
 \tag{5.26}$$

$$\begin{aligned}
 [E] \{\Phi_0(\sigma)\} + [F] \frac{\sigma^2+m}{\sigma(1-m\sigma^2)} \{\overline{\Phi_0(\sigma)}\}' + [G] \frac{1}{R^2(1-m\sigma^2)^2} \{\overline{\Phi_0(\sigma)}\}'' \\
 - [G] \frac{2m\sigma^3}{R^2(1-m\sigma^2)^3} \{\overline{\Phi_0(\sigma)}\}' + [H] \{\overline{\Psi_0(\sigma)}\} = \{Q^0\}.
 \end{aligned}
 \tag{5.27}$$

$$\begin{aligned}
 \{Q^0\} = \{Q\} - [E] \left\{ \frac{C}{B} \right\} \ln \sigma - R [E] \left\{ \frac{\phi_1}{\beta_1} \right\} \sigma - [F] \left\{ \frac{\overline{C}}{\overline{B}} \right\} \frac{\sigma^2+m}{1-m\sigma^2} \\
 - R [F] \left\{ \frac{\phi_1}{\beta_1} \right\} \frac{\sigma^2+m}{\sigma(1-m\sigma^2)} + [G] \left\{ \frac{\overline{C}}{\overline{B}} \right\} \frac{\sigma^2}{R^2(1-m\sigma^2)^2} \\
 + [G] \left\{ \frac{\overline{C}}{\overline{B}} \right\} \frac{2m\sigma^4}{R^2(1-m\sigma^2)^3} + R [G] \left\{ \frac{\phi_1}{\beta_1} \right\} \frac{2m\sigma^3}{R^2(1-m\sigma^2)^3} \\
 + [H] \left\{ \frac{\overline{B}_1}{B} \right\} \ln \sigma - R [H] \left\{ \frac{\overline{\psi}_1}{2\overline{\alpha}_2} \right\} \frac{1}{\sigma}.
 \end{aligned}
 \tag{5.28}$$

For an infinite plate with an elliptical hole, we suppose $\phi_0(\infty) = 0$ and $\beta_0(\infty) = 0$, namely

$$\{\Phi_0(\infty)\} = 0.
 \tag{5.29}$$

The function $\{\Phi_0(\eta)\}$, which is holomorphic outside the unit circle, can be expanded as

$$\{\Phi_0(\eta)\} = \sum_{k=1}^{\infty} \{\Phi_k\} \eta^{-k},
 \tag{5.30}$$

where $\{\Phi_k\}$ is a constant coefficient array and hence

$$\{\Phi_0(\eta)\}' = - \sum_{k=1}^{\infty} k \{\Phi_k\} \eta^{-k-1}, \quad \{\Phi_0(\eta)\}'' = \sum_{k=1}^{\infty} k(k+1) \{\Phi_k\} \eta^{-k-2}.
 \tag{5.31}$$

By rewriting Eq. (5.25) in terms of Cauchy integral, that is, by multiplying each term in Eq. (5.25) with $\frac{d\sigma}{2\pi i(\sigma-\eta)}$ where $|\eta| > 1$ and then integrating along γ , we can find

$$\begin{aligned}
 & -[F]\eta \frac{1+m\eta^2}{\eta^2-m} \{\Phi_0(\eta)\}' - [G] \frac{\eta^4}{R^2(\eta^2-m)^2} \{\Phi_0(\eta)\}'' \\
 & + [G] \frac{2m\eta^3}{R^2(\eta^2-m)^3} \{\Phi_0(\eta)\}' - [H]\{\Psi_0(\eta)\} + [H]\{\Psi_0(\infty)\} = \frac{1}{2\pi i} \int_{\gamma} \frac{\{\bar{Q}^0\} d\sigma}{\sigma-\eta}. \quad (5.32)
 \end{aligned}$$

from which we can obtain the expression of $\{\Psi_0(\eta)\}$ once the function $\Phi_0(\eta)$ and the integral at the right-hand side are known. Notice that the term $\{\Psi_0(\infty)\}$ may be omitted since it has no effect on the resultant forces in the plate.

Now let us examine Eq. (5.27), which is conjugate to Eq. (5.25). Rewriting Eq. (5.27) in terms of Cauchy integral eventually leads to

$$-[E]\{\Phi_0(\eta)\} = \frac{1}{2\pi i} \int_{\gamma} \frac{\{Q^0\} d\sigma}{\sigma-\eta}, \quad |\eta| > 1. \quad (5.33)$$

from which we can obtain the expression of $\{\Phi_0(\eta)\}$ once the Cauchy integral of $\{Q^0\}$ is known. In the following, the two integrals at the right-hand sides of Eqs. (5.32) and (5.33) will be calculated. The calculation is either easy or complex, depending on the nature of the problem studied.

6 An infinite plate with an elliptical hole subject to loads at infinity

We consider a plate with a free elliptical hole, but subject to loads $N_1, N_2, N_{12}, M_1, M_2, M_{12}$ at infinity. It can be found that $f_1 - if_2 = 0, f_3 - if_4 = 0, C = 0, B = 0,$ and $B_1 = 0.$ Suppose the angle between the direction of N_1 and the x -axis is Θ and N_2 is perpendicular to $N_1.$ The following transform relations between Cartesian coordinates and curvilinear coordinates shall be adopted

$$\begin{aligned}
 N_x^\infty + N_y^\infty &= N_1 + N_2, & N_y^\infty - N_x^\infty + 2iN_{xy}^\infty &= (N_2 - N_1 + 2iN_{12}) e^{-2i\Theta}, \\
 M_x^\infty + M_y^\infty &= M_1 + M_2, & M_y^\infty - M_x^\infty + 2iM_{xy}^\infty &= (M_2 - M_1 + 2iM_{12}) e^{-2i\Theta}. \quad (6.1)
 \end{aligned}$$

Notice the following expressions (see Yang et al. [21])

$$\begin{Bmatrix} \phi_1 \\ \beta_1 \end{Bmatrix} = \frac{1}{2} [D]^{-1} \begin{Bmatrix} N_x^\infty + N_y^\infty \\ M_x^\infty + M_y^\infty \end{Bmatrix}, \quad \begin{Bmatrix} \psi_1 \\ 2\alpha_2 \end{Bmatrix} = [H]^{-1} \begin{Bmatrix} N_y^\infty - N_x^\infty + 2iN_{xy}^\infty \\ M_y^\infty - M_x^\infty + 2iM_{xy}^\infty \end{Bmatrix}. \quad (6.2)$$

Therefore

$$\begin{Bmatrix} \phi_1 \\ \beta_1 \end{Bmatrix} = \frac{1}{2} [D]^{-1} \begin{Bmatrix} N_1 + N_2 \\ M_1 + M_2 \end{Bmatrix}, \quad \begin{Bmatrix} \psi_1 \\ 2\alpha_2 \end{Bmatrix} = [H]^{-1} \begin{Bmatrix} N_2 - N_1 + 2iN_{12} \\ M_2 - M_1 + 2iM_{12} \end{Bmatrix} e^{-2i\Theta}, \quad (6.3)$$

where $[D] = \begin{bmatrix} a_1 & 4a_2 \\ -b_1 & 4b_2 \end{bmatrix}.$ Hence, the constants $\phi_1, \beta_1, \alpha_2$ and ψ_1 can be completely determined.

The following Cauchy integrals can be calculated from Eqs. (5.26) and (5.28)

$$\begin{aligned}
 \frac{1}{2\pi i} \int_{\gamma} \frac{\{\bar{Q}^0\}}{\sigma-\eta} d\sigma &= R[E] \frac{1}{\eta} \begin{Bmatrix} \phi_1 \\ \beta_1 \end{Bmatrix} + R[F] \begin{Bmatrix} \phi_1 \\ \beta_1 \end{Bmatrix} \frac{(1+m^2)\eta}{\eta^2-m} \\
 & - \frac{2m}{R} [G] \begin{Bmatrix} \phi_1 \\ \beta_1 \end{Bmatrix} \frac{\eta^3}{(\eta^2-m)^3}, \quad |\eta| > 1. \quad (6.4)
 \end{aligned}$$

$$\frac{1}{2\pi i} \int_{\gamma} \frac{\{Q^0\}}{\sigma-\eta} d\sigma = Rm[F] \begin{Bmatrix} \phi_1 \\ \beta_1 \end{Bmatrix} \frac{1}{\eta} + R[H] \begin{Bmatrix} \bar{\psi}_1 \\ 2\bar{\alpha}_2 \end{Bmatrix} \frac{1}{\eta}, \quad |\eta| > 1. \quad (6.5)$$

By substituting Eq. (6.5) into (5.33), we obtain

$$\{\Phi_0(\eta)\} = R \{\gamma^0\} \frac{1}{\eta}, \tag{6.6}$$

where

$$\{\gamma^0\} = -m [E]^{-1} [F] \begin{Bmatrix} \phi_1 \\ \beta_1 \end{Bmatrix} - [E]^{-1} [H] \begin{Bmatrix} \bar{\psi}_1 \\ 2\bar{\alpha}_2 \end{Bmatrix}. \tag{6.7}$$

By substituting Eqs. (6.4) and (6.6) into Eq. (5.32) and omitting the constant terms, we obtain

$$\begin{aligned} \{\Psi_0(\eta)\} = & R [H]^{-1} [F] \{\gamma^0\} \frac{1+m\eta^2}{\eta(\eta^2-m)} - \frac{2}{R} [H]^{-1} [G] \{\gamma^0\} \frac{\eta^3}{(\eta^2-m)^3} - \\ & \left(R [H]^{-1} [E] \frac{1}{\eta} + R(1+m^2) [H]^{-1} [F] \frac{\eta}{\eta^2-m} - \frac{2m}{R} [H]^{-1} [G] \frac{\eta^3}{(\eta^2-m)^3} \right) \begin{Bmatrix} \phi_1 \\ \beta_1 \end{Bmatrix}. \end{aligned} \tag{6.8}$$

Substituting Eqs. (6.6) and (6.8) into Eqs. (5.19) and (5.20) leads to

$$\{\Phi(\eta)\} = R \begin{Bmatrix} \phi_1 \\ \beta_1 \end{Bmatrix} \eta + R \{\gamma^0\} \frac{1}{\eta}. \tag{6.9}$$

$$\begin{aligned} \{\Psi(\eta)\} = & R \begin{Bmatrix} \psi_1 \\ 2\alpha_2 \end{Bmatrix} \eta + R [H]^{-1} [F] \{\gamma^0\} \frac{1+m\eta^2}{\eta(\eta^2-m)} - \frac{2}{R} [H]^{-1} [G] \{\gamma^0\} \frac{\eta^3}{(\eta^2-m)^3} - \\ & \left(R [H]^{-1} [E] \frac{1}{\eta} + R(1+m^2) [H]^{-1} [F] \frac{\eta}{\eta^2-m} - \frac{2m}{R} [H]^{-1} [G] \frac{\eta^3}{(\eta^2-m)^3} \right) \begin{Bmatrix} \phi_1 \\ \beta_1 \end{Bmatrix}. \end{aligned} \tag{6.10}$$

The resultant forces and moments in the plate can be expressed in the following matrix form

$$\begin{Bmatrix} N_x + N_y \\ M_x + M_y \end{Bmatrix} = 2 [D] \operatorname{Re} \{ \Phi(\zeta) \}' , \tag{6.11}$$

$$\begin{Bmatrix} N_y - N_x + 2iN_{xy} \\ M_y - M_x + 2iM_{xy} \end{Bmatrix} = [F] \bar{\zeta} \{ \Phi(\zeta) \}'' + [G] \{ \Phi(\zeta) \}''' + [H] \{ \Psi(\zeta) \}' , \tag{6.12}$$

where $\{ \Phi(\zeta) \}' = \{ \Phi(\eta) \}' / \omega'(\eta)$.

It is very simple to evaluate the resultant forces on the boundary of the hole. The polar coordinates are adopted here to describe a point in the complex plane η , namely $\eta = \rho e^{i\theta}$. $\rho = 1$ corresponds to the unit circle and also the boundary of the elliptical hole. Coordinates ρ and θ can be interpreted as curvilinear coordinates in the plane η . By making use of the relations $N_\rho + N_\theta = N_x + N_y$ and $M_\rho + M_\theta = M_x + M_y$, we find $N_\rho = 0$ and $M_\rho = 0$ on the boundary of the hole and

$$\begin{Bmatrix} N_\theta \\ M_\theta \end{Bmatrix} = 2 [D] \operatorname{Re} \left(\{ \Phi(\eta) \}' \frac{\eta^2}{R(\eta^2-m)} \right)_{\rho=1}. \tag{6.13}$$

Substituting Eq. (6.9) into Eq. (6.13) leads to

$$\begin{Bmatrix} N_\theta \\ M_\theta \end{Bmatrix} = 2 [D] \operatorname{Re} \left\{ \left(\begin{Bmatrix} \phi_1 \\ \beta_1 \end{Bmatrix} - \{\gamma^0\} e^{-2i\theta} \right) \frac{e^{2i\theta}}{e^{2i\theta} - m} \right\}. \tag{6.14a}$$

By substituting Eqs. (6.7) and (6.3) into (6.14a) and noticing the relationship $[F] = 2[D] - [E]$, we obtain

$$\begin{aligned} \begin{Bmatrix} N_\theta \\ M_\theta \end{Bmatrix} = & \operatorname{Re} \left\{ \begin{Bmatrix} N_1 + N_2 \\ M_1 + M_2 \end{Bmatrix} + 2 [D] [E]^{-1} \left(m \begin{Bmatrix} N_1 + N_2 \\ M_1 + M_2 \end{Bmatrix} + \right. \right. \\ & \left. \left. \begin{Bmatrix} N_2 - N_1 - 2iN_{12} \\ M_2 - M_1 - 2iM_{12} \end{Bmatrix} e^{2i\theta} \right) \frac{e^{-2i\theta} - m}{1 - 2m \cos 2\theta + m^2} \right\}. \end{aligned} \tag{6.14b}$$

That is

$$\begin{aligned} \begin{Bmatrix} N_\theta \\ M_\theta \end{Bmatrix} &= \begin{Bmatrix} N_1 + N_2 \\ M_1 + M_2 \end{Bmatrix} + 2[D][E]^{-1} \left(\begin{Bmatrix} N_1 + N_2 \\ M_1 + M_2 \end{Bmatrix} (m \cos 2\theta - m^2) + \right. \\ &\quad \left. \begin{Bmatrix} N_2 - N_1 \\ M_2 - M_1 \end{Bmatrix} [\cos 2(\Theta - \theta) - m \cos 2\Theta] + \right. \\ &\quad \left. 2 \begin{Bmatrix} N_{12} \\ M_{12} \end{Bmatrix} [\sin 2(\Theta - \theta) - m \sin 2\Theta] \right) \frac{1}{1 - 2m \cos 2\theta + m^2}. \end{aligned} \quad (6.14c)$$

Let $[D][E]^{-1} = (d_{ij}^e)$, in which

$$\begin{aligned} d_{11}^e &= 1, \quad d_{12}^e = 0, \quad d_{21}^e = (b_1 b_6 + 4a_6 b_2)/J, \quad d_{22}^e = 4(a_1 b_2 + a_2 b_1)/J, \\ J &= a_1(8b_2 - b_6) + 4a_2(2b_1 + a_6). \end{aligned} \quad (6.15)$$

We can find from Eqs. (6.14c) and (6.15) that N_θ on the boundary of the hole is independent of M_1 , M_2 , M_{12} and the material constants. Its expression is as follows

$$\begin{aligned} N_\theta &= \frac{1}{1 - 2m \cos 2\theta + m^2} \{ (1 - m^2)(N_1 + N_2) + 2[\cos 2(\Theta - \theta) - m \cos 2\Theta](N_2 - N_1) \\ &\quad + 4[\sin 2(\Theta - \theta) - m \sin 2\Theta]N_{12} \}. \end{aligned} \quad (6.16)$$

For a single load, we may define the resultant force concentration factors (RFCFs) K_{ij} as follows

$$K_{i1} = N_{\theta \max}(a, \theta)/N, \quad K_{i2} = M_{\theta \max}(a, \theta)/M, \quad (i = 1, 2, 3). \quad (6.17)$$

where $i = 1$ corresponds to uniaxial tension ($N = N_1$, $M_1 = 0$) or cylindrical bending ($M = M_1$, $N_1 = 0$); $i = 2$ to equi-biaxial tension ($N = N_1 = N_2$, $M_1 = M_2 = 0$) or pure bending ($M = M_1 = M_2$, $N_1 = N_2 = 0$); and $i = 3$ to pure shear ($N = N_{12}$, $M_{12} = 0$) or pure torsion ($M = M_{12}$, $N_{12} = 0$). In the following, six special cases will be discussed.

6.1 Uniaxial tension

In this case, we have $N_1 = N$, $N_2 = N_{12} = 0$. It can be obtained from Eq. (6.16) that

$$N_\theta = \frac{1 - m^2 - 2 \cos 2(\Theta - \theta) + 2m \cos 2\Theta}{1 - 2m \cos 2\theta + m^2} N, \quad (6.18)$$

which is the same as the result that is obtained by integrating along the thickness direction the stress component σ_θ in an isotropic and homogeneous plate as in Muskhelishvili [1]. When $N_1 = N$ is perpendicular to the major axis of the elliptical hole (namely $\Theta = \pi/2$), it can be found from Eq. (6.18) that the maximum N_θ appears at $\theta = 0$ and $\theta = \pi$ (namely both ends of the major axis) with its value being

$$(N_\theta)_{\max} = \frac{3 + m}{1 - m} N = \left(1 + 2\frac{a}{b}\right) N. \quad (6.19)$$

Therefore, the resultant force concentration factor is $K_{11} = 1 + 2a/b$. It means that the more flat the elliptical hole, the greater the K_{11} . K_{11} will tend to infinity as $b \rightarrow 0$.

6.2 Equi-biaxial tension

In this case, we have $N_1 = N_2 = N$, and $N_{12} = 0$. It can be obtained from Eq. (6.16) that

$$N_\theta = \frac{2(1 - m^2)N}{1 - 2m \cos 2\theta + m^2}, \quad (6.20)$$

which shows that the maximum N_θ appears at $\theta = 0$ and $\theta = \pi$ with the value being

$$(N_\theta)_{\max} = 2\frac{1 + m}{1 - m} N = 2\frac{a}{b} N. \quad (6.21)$$

Therefore, the resultant force concentration factor is $K_{21} = 2a/b$.

6.3 Pure shear

In this case, we have $N_{12} = N$, and $N_1 = N_2 = 0$. It can be obtained from Eq. (6.16) that

$$N_\theta = \frac{4[\sin 2(\Theta - \theta) - m \sin 2\Theta]}{1 - 2m \cos 2\theta + m^2} N, \quad (6.22)$$

which shows that N_θ is dependent of θ and Θ . When $\Theta = 0$, the extremum of N_θ occurs at $\theta = \pm\theta_0$ and $\theta = \pi \pm \theta_0$, where $\cos 2\theta_0 = 2m/(1 + m^2)$ and $\sin 2\theta_0 = (1 - m^2)/(1 + m^2)$. The extrema are given by

$$(N_\theta)_{\text{extremum}} = \mp \frac{4N}{1 - m^2}. \quad (6.23)$$

Therefore, the resultant force concentration factor is $K_{31} = 4/(1 - m^2) = 2 + a/b + b/a$.

6.4 Cylindrical bending ($\Theta = \pi/2$)

In this case, we have $M_1 = M$, $M_2 = M_{12} = 0$, and $N_1 = N_2 = N_{12} = 0$. It can be obtained from Eq. (6.14c) that

$$M_\theta = M + \frac{2(1 + m) M d_{22}^e (\cos 2\theta - m)}{1 + m^2 - 2m \cos 2\theta}, \quad (6.24)$$

which shows that the maximum M_θ occurs at $\theta = 0$ and $\theta = \pi$ and the resultant force concentration factor is $K_{12} = 1 + 2d_{22}^e(1 + m)/(1 - m) = 1 + 2d_{22}^e a/b$.

6.5 Pure bending

In this case, we have $M_1 = M_2 = M$, $M_{12} = 0$, and $N_1 = N_2 = N_{12} = 0$. It can be obtained from Eq. (6.14c) that

$$M_\theta = 2M + \frac{4m M d_{22}^e (\cos 2\theta - m)}{1 + m^2 - 2m \cos 2\theta}, \quad (6.25)$$

which indicates that M_θ reaches its maximum at $\theta = 0$ and $\theta = \pi$ with the resultant force concentration factor $K_{22} = 2 + 4d_{22}^e m/(1 - m) = 2 - 2d_{22}^e(1 - a/b)$.

6.6 Pure torsion ($\Theta = 0$)

In this case, we have $M_1 = M_2 = 0$, $M_{12} = M$, and $N_1 = N_2 = N_{12} = 0$. It can be obtained from Eq. (6.14c) that

$$M_\theta = -\frac{4M d_{22}^e \sin 2\theta}{1 + m^2 - 2m \cos 2\theta}. \quad (6.26)$$

This expression indicates that M_θ obtains its extremum at $\theta = \frac{1}{2} \arccos [2m/(1 + m^2)]$ with the resultant force concentration factor $K_{32} = d_{22}^e(2 + a/b + b/a)$.

For a circular hole, we have $m = 0$ and $\Theta = 0$. In this case, we find that Eq. (6.14b) is exactly the same as Eq. (7.5) in Yang et al. [21].

7 An infinite plate with an elliptical hole subject to loads on the boundary of the hole

7.1 Uniform loads applied on the boundary of the hole

We consider an infinite plate subject to loads N_n^b , N_{nt}^b , M_n^b and M_{nt}^b applied uniformly on the boundary of the elliptical hole. No loads are applied at infinity. In this case, we know that the constants ϕ_1 , β_1 , α_2 and ψ_1 are all zero. The loads applied on the boundary of the elliptical hole should constitute a balanced system of forces,

requiring that the principal force vector and principal moment be zero. Thus, we have $C = 0$, $B = 0$, and $B_1 = 0$. By making use of Eq. (4.2)₂ and $Q_n^b(s) = 0$, we obtain from Eqs. (4.15)₁ and (4.16)₁ that

$$f_1 - if_2 = 2 \int \left[N_n^b(s) - iN_{nt}^b(s) \right] d\bar{\zeta} = 2R \left(N_n^b - iN_{nt}^b \right) \left(\frac{1}{\sigma} + m\sigma \right). \quad (7.1)$$

$$f_3 - if_4 = 2 \int \left[M_n^b(s) - iP(s) \right] d\bar{\zeta} = 2R \left(M_n^b - iM_{nt}^b \right) \left(\frac{1}{\sigma} + m\sigma \right). \quad (7.2)$$

It can be found from Eqs. (5.26) and (5.28) that

$$\{\bar{Q}^0\} = \{\bar{Q}\} = \begin{Bmatrix} f_1 - if_2 \\ f_3 - if_4 \end{Bmatrix} = 2R \begin{Bmatrix} N_n^b - iN_{nt}^b \\ M_n^b - iM_{nt}^b \end{Bmatrix} \left(\frac{1}{\sigma} + m\sigma \right). \quad (7.3)$$

$$\{Q^0\} = \begin{Bmatrix} f_1 + if_2 \\ f_3 + if_4 \end{Bmatrix} = 2R \begin{Bmatrix} N_n^b + iN_{nt}^b \\ M_n^b + iM_{nt}^b \end{Bmatrix} \left(\frac{m}{\sigma} + \sigma \right). \quad (7.4)$$

Hence

$$\frac{1}{2\pi i} \int_{\gamma} \frac{\{\bar{Q}^0\} d\sigma}{\sigma - \eta} = -2 \frac{R}{\eta} \begin{Bmatrix} N_n^b - iN_{nt}^b \\ M_n^b - iM_{nt}^b \end{Bmatrix}, \quad \frac{1}{2\pi i} \int_{\gamma} \frac{\{Q^0\} d\sigma}{\sigma - \eta} = -2 \frac{mR}{\eta} \begin{Bmatrix} N_n^b + iN_{nt}^b \\ M_n^b + iM_{nt}^b \end{Bmatrix}. \quad (7.5)$$

Substituting Eq. (7.5)₂ into Eq. (5.33) gives

$$\{\Phi_0(\eta)\} = R \{\gamma^1\} \frac{1}{\eta}, \quad (7.6)$$

in which

$$\{\gamma^1\} = 2m [E]^{-1} \begin{Bmatrix} N_n^b + iN_{nt}^b \\ M_n^b + iM_{nt}^b \end{Bmatrix}^T. \quad (7.7)$$

Substituting Eqs. (7.5)₁ and (7.6) into Eq. (5.32) leads to

$$\begin{aligned} \{\Psi_0(\eta)\} &= 2 \frac{R}{\eta} [H]^{-1} \begin{Bmatrix} N_n^b - iN_{nt}^b \\ M_n^b - iM_{nt}^b \end{Bmatrix}^T + R [H]^{-1} [F] \{\gamma^1\} \frac{1+m\eta^2}{\eta(\eta^2-m)} \\ &\quad - \frac{2m}{R} [H]^{-1} [G] \{\gamma^1\} \frac{\eta}{(\eta^2-m)^3} - \frac{2}{R} [H]^{-1} [G] \{\gamma^1\} \frac{\eta}{(\eta^2-m)^2}. \end{aligned} \quad (7.8)$$

Therefore, we can obtain from Eqs. (5.19) and (5.20) that

$$\{\Phi(\eta)\} = \{\Phi_0(\eta)\}, \quad \{\Psi(\eta)\} = \{\Psi_0(\eta)\}, \quad (7.9)$$

where the expressions of $\Phi_0(\eta)$ and $\Psi_0(\eta)$ are shown in Eqs. (7.6) and (7.8).

7.2 Uniform loads applied on part of boundary of the hole

We now consider the case that uniform loads N_n^b , N_{nt}^b , M_n^b and M_{nt}^b are applied only on the arc t_1t_2 of the boundary of the elliptical hole where t_1 and t_2 correspond to the points σ_1 and σ_2 on the boundary of the unit circle hole, as shown in Fig. 3. Meanwhile, no loads are applied at infinity, which ensures that the constants ϕ_1 , β_1 , α_2 and ψ_1 are all zero. By starting from the point t_1 and calculating the line integral in a clockwise manner, just as Eqs. (7.1) and (7.2), we find that

$$\begin{aligned} f_1 - if_2 &= 0, \quad t \text{ on the arc } t_1Mt_2, \\ f_1 - if_2 &= 2 \left(N_n^b - iN_{nt}^b \right) (\bar{t} - \bar{t}_2), \quad t \text{ on the arc } t_2t_1, \end{aligned} \quad (7.10)$$

$$\begin{aligned} f_3 - if_4 &= 0, \quad t \text{ on the arc } t_1Mt_2, \\ f_3 - if_4 &= 2 \left(M_n^b - iM_{nt}^b \right) (\bar{t} - \bar{t}_2), \quad t \text{ on the arc } t_2t_1. \end{aligned} \quad (7.11)$$

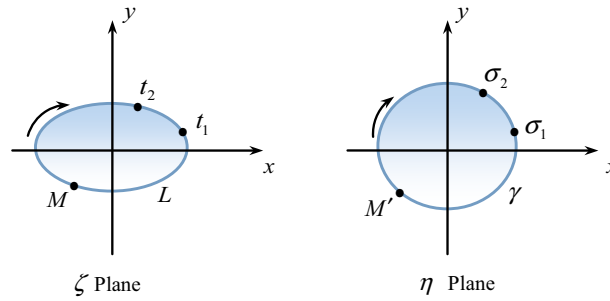


Fig. 3 Schematic diagram of an elliptic hole

By virtue of Eqs. (3.10)₁ and (3.12)₁ in Yang et al. [21], we obtain the following expressions of the principal vectors and moments

$$\begin{aligned}
 X - iY &= \int_{t_2}^{t_1} [N_{xn}^b(s) - iN_{yn}^b(s)] ds = i \int_{t_2}^{t_1} (N_n^b - iN_{nt}^b) d\bar{\zeta} = i (N_n^b - iN_{nt}^b) (\bar{t}_1 - \bar{t}_2), \quad (7.12) \\
 M_X - iM_Y &= -i \int_{t_2}^{t_1} [M_{xn}^b(s) - iM_{yn}^b(s)] ds = \int_{t_2}^{t_1} (M_n^b - iM_{nt}^b) d\bar{\zeta} = (M_n^b - iM_{nt}^b) (\bar{t}_1 - \bar{t}_2), \quad (7.13)
 \end{aligned}$$

where

$$t_1 = R \left(\sigma_1 + \frac{m}{\sigma_1} \right), \quad t_2 = R \left(\sigma_2 + \frac{m}{\sigma_2} \right). \quad (7.14)$$

As a result, Eqs. (5.26) and (5.28) can be simplified to

$$\begin{aligned}
 \{\bar{Q}^0\} &= \left\{ \begin{matrix} f_1 - if_2 \\ f_3 - if_4 \end{matrix} \right\} + [E] \left\{ \begin{matrix} \bar{C} \\ \bar{B} \end{matrix} \right\} \ln \sigma - [F] \left\{ \begin{matrix} C \\ B \end{matrix} \right\} \frac{1+m\sigma^2}{\sigma^2 - m} + \\
 [G] \left\{ \begin{matrix} C \\ B \end{matrix} \right\} \frac{\sigma^2}{R^2(\sigma^2 - m)^2} &+ [G] \left\{ \begin{matrix} C \\ B \end{matrix} \right\} \frac{2m\sigma^2}{R^2(\sigma^2 - m)^3} - [H] \left\{ \begin{matrix} B_1 \\ \bar{B} \end{matrix} \right\} \ln \sigma, \quad (7.15)
 \end{aligned}$$

$$\begin{aligned}
 \{Q^0\} &= \left\{ \begin{matrix} f_1 + if_2 \\ f_3 + if_4 \end{matrix} \right\} - [E] \left\{ \begin{matrix} C \\ B \end{matrix} \right\} \ln \sigma - [F] \left\{ \begin{matrix} \bar{C} \\ \bar{B} \end{matrix} \right\} \frac{\sigma^2 + m}{1 - m\sigma^2} + \\
 [G] \left\{ \begin{matrix} \bar{C} \\ \bar{B} \end{matrix} \right\} \frac{\sigma^2}{R^2(1 - m\sigma^2)^2} &+ [G] \left\{ \begin{matrix} \bar{C} \\ \bar{B} \end{matrix} \right\} \frac{2m\sigma^4}{R^2(1 - m\sigma^2)^3} + [H] \left\{ \begin{matrix} \bar{B}_1 \\ B \end{matrix} \right\} \ln \sigma, \quad (7.16)
 \end{aligned}$$

where the constants C, B, B_1 can be determined from Eqs. (4.23), (7.12) and (7.13), respectively; $f_1 - if_2$ and $f_3 - if_4$ can be determined from Eqs. (7.10) and (7.11), respectively.

By rewriting Eqs. (7.15) and (7.16) in terms of Cauchy integrals and then integrating along γ , omitting the constant terms that are irrelevant to the resultants forces, we can obtain

$$\begin{aligned}
 \frac{1}{2\pi i} \int_{\gamma} \frac{\{\bar{Q}^0\}}{\sigma - \eta} d\sigma &= \frac{R}{\pi i} \left\{ \begin{matrix} N_n^b - iN_{nt}^b \\ M_n^b - iM_{nt}^b \end{matrix} \right\} \left[-\frac{1}{\eta} \ln \frac{\sigma_2}{\sigma_1} + \left(\frac{1}{\eta} + m\eta \right) \ln \frac{\sigma_2 - \eta}{\sigma_1 - \eta} \right] \\
 - \frac{\bar{t}_2}{\pi i} \left\{ \begin{matrix} N_n^b - iN_{nt}^b \\ M_n^b - iM_{nt}^b \end{matrix} \right\} \ln \frac{\sigma_2 - \eta}{\sigma_1 - \eta} &+ [F] \left\{ \begin{matrix} C \\ B \end{matrix} \right\} \frac{1+m\eta^2}{\eta^2 - m} \\
 + \left([E] \left\{ \begin{matrix} \bar{C} \\ \bar{B} \end{matrix} \right\} - [H] \left\{ \begin{matrix} B_1 \\ \bar{B} \end{matrix} \right\} \right) &[\ln(\sigma_1 - \eta) - \ln \eta] \\
 - [G] \left\{ \begin{matrix} C \\ B \end{matrix} \right\} \frac{\eta^2}{R^2(\eta^2 - m)^2} &- [G] \left\{ \begin{matrix} C \\ B \end{matrix} \right\} \frac{2m\eta^2}{R^2(\eta^2 - m)^3}. \quad (7.17)
 \end{aligned}$$

$$\begin{aligned} \frac{1}{2\pi i} \int_{\gamma} \frac{\{Q^0\}}{\sigma - \eta} d\sigma &= \frac{R}{\pi i} \left\{ \begin{matrix} N_n^b + iN_{nt}^b \\ M_n^b + iM_{nt}^b \end{matrix} \right\} \left[-\frac{m}{\eta} \ln \frac{\sigma_2}{\sigma_1} + \left(\eta + \frac{m}{\eta} \right) \ln \frac{\sigma_2 - \eta}{\sigma_1 - \eta} \right] \\ &- \frac{t_2}{\pi i} \left\{ \begin{matrix} N_n^b + iN_{nt}^b \\ M_n^b + iM_{nt}^b \end{matrix} \right\} \ln \frac{\sigma_2 - \eta}{\sigma_1 - \eta} \\ &+ \left([H] \left\{ \begin{matrix} \bar{B}_1 \\ B \end{matrix} \right\} - [E] \left\{ \begin{matrix} C \\ B \end{matrix} \right\} \right) [\ln(\sigma_1 - \eta) - \ln \eta]. \end{aligned} \quad (7.18)$$

Substituting Eq. (7.18) into Eq. (5.33) yields

$$\begin{aligned} \{\phi_0(\eta)\} &= -\frac{R}{\pi i} [E]^{-1} \left\{ \begin{matrix} N_n^b + iN_{nt}^b \\ M_n^b + iM_{nt}^b \end{matrix} \right\} \left[-\frac{m}{\eta} \ln \frac{\sigma_2}{\sigma_1} + \left(\eta + \frac{m}{\eta} \right) \ln \frac{\sigma_2 - \eta}{\sigma_1 - \eta} \right] \\ &+ \frac{t_2}{\pi i} [E]^{-1} \left\{ \begin{matrix} N_n^b + iN_{nt}^b \\ M_n^b + iM_{nt}^b \end{matrix} \right\} \ln \frac{\sigma_2 - \eta}{\sigma_1 - \eta} - \left([E]^{-1} [H] \left\{ \begin{matrix} \bar{B}_1 \\ B \end{matrix} \right\} - \left\{ \begin{matrix} C \\ B \end{matrix} \right\} \right) [\ln(\sigma_1 - \eta) - \ln \eta]. \end{aligned} \quad (7.19)$$

Substituting Eq. (7.17) into Eq. (5.32) gives

$$\begin{aligned} \{\Psi_0(\eta)\} &= -\frac{R}{\pi i} [H]^{-1} \left\{ \begin{matrix} N_n^b - iN_{nt}^b \\ M_n^b - iM_{nt}^b \end{matrix} \right\} \left[-\frac{1}{\eta} \ln \frac{\sigma_2}{\sigma_1} + \left(\frac{1}{\eta} + m\eta \right) \ln \frac{\sigma_2 - \eta}{\sigma_1 - \eta} \right] \\ &+ \frac{\bar{t}_2}{\pi i} [H]^{-1} \left\{ \begin{matrix} N_n^b - iN_{nt}^b \\ M_n^b - iM_{nt}^b \end{matrix} \right\} \ln \frac{\sigma_2 - \eta}{\sigma_1 - \eta} - [H]^{-1} [F] \left\{ \begin{matrix} C \\ B \end{matrix} \right\} \frac{1+m\eta^2}{\eta^2 - m} \\ &- [H]^{-1} \left([E] \left\{ \begin{matrix} C \\ B \end{matrix} \right\} - [H] \left\{ \begin{matrix} B_1 \\ B \end{matrix} \right\} \right) [\ln(\sigma_1 - \eta) - \ln \eta] \\ &+ [H]^{-1} [G] \left\{ \begin{matrix} C \\ B \end{matrix} \right\} \frac{\eta^2}{R^2 (\eta^2 - m)^2} + [H]^{-1} [G] \left\{ \begin{matrix} C \\ B \end{matrix} \right\} \frac{2m\eta^2}{R^2 (\eta^2 - m)^3} \\ &- [H]^{-1} [G] \frac{\eta^4}{R^2 (\eta^2 - m)^2} \{\phi_0(\eta)\}'' \\ &+ [H]^{-1} \left([G] \frac{2m\eta^3}{R^2 (\eta^2 - m)^3} - [F] \eta \frac{1+m\eta^2}{\eta^2 - m} \right) \{\phi_0(\eta)\}'. \end{aligned} \quad (7.20)$$

It can be obtained from Eqs. (5.19) and (5.20) that

$$\{\phi(\eta)\} = \left\{ \begin{matrix} C \\ B \end{matrix} \right\} \ln \eta + \{\phi_0(\eta)\}, \quad \{\Psi(\eta)\} = \left\{ \begin{matrix} B_1 \\ B \end{matrix} \right\} \ln \eta + \{\Psi_0(\eta)\}, \quad (7.21)$$

where the expressions of $\phi_0(\eta)$ and $\Psi_0(\eta)$ are shown in Eqs. (7.19) and (7.20).

If the uniform loads are applied over the total boundary of the elliptical hole, we have

$$t_1 = t_2, \quad \sigma_1 = \sigma_2, \quad \ln \frac{\sigma_2}{\sigma_1} = 2\pi i. \quad (7.22)$$

Consequently, Eq. (7.21) becomes identical with Eq. (7.9).

With the above solution in hand, the problem of any concentrated force applied on the boundary of the elliptical hole can be solved by illimitably reducing the size of the arc $t_1 t_2$ while increasing the load magnitude. Similarly, it is very convenient to obtain the analytical solution when an arbitrary number of concentrated forces of any magnitude applied on the boundary of the elliptical hole.

8 Numerical results and discussions

Consider an infinite FGM plate containing an elliptical hole subject to a uniform pressure N_n^b applied on the edge of the elliptical hole. Let $h = 0.2\text{m}$. The material parameters of the infinite plate are assumed to be of the form (Yang et al. [12])

$$c_{ij} = c_{ij}^0 e^{\frac{(z + h/2)}{h} \lambda}, \quad (i, j = 1, 2, \dots, 6), \quad (8.1)$$

where c_{ij}^0 are material parameters at $z = -h/2$ which are given in Table 1. The parameter λ is the gradient index reflecting the degree of material inhomogeneity. Obviously, $\lambda = 0$ corresponds to homogeneous materials.

The hole in the plate has an important effect on the strength of the plate. The following results will focus on the impact of the gradient index λ and the shape of the hole a/b on the stress field in the plate. Unless stated otherwise, we take $\theta = 0$, $a = 1\text{m}$, and $z = h/2$.

Figure 4 shows the distribution of the normalized hoop stress σ_θ/σ in the ρ -direction for $a/b = 2$ and different values of λ . It is noted that $\sigma = N_n^b/h$, and $\rho = 1$ corresponds to the boundary of the elliptical hole. We can find that the maximum absolute value of the normalized hoop stress at the boundary of the elliptical hole occurs when $\lambda = 2$ and the minimum absolute value is obtained when $\lambda = -2$. There is a clear inflection point at $\rho = 1.5$ for all three curves in the figure. As expected, the normalized hoop stress tends to zero at infinity.

Figure 5 depicts the distribution of the normalized hoop stress σ_θ/σ at $\rho = 1.5$ in the θ -direction for $a/b = 2$ and different values of λ . It can be found that the distribution of the normalized hoop stress for $\lambda = 2$ is not the same as that for $\lambda = 0$ and $\lambda = -2$. The line of $\theta = \pi/2$ and $\theta = 3\pi/2$ is the line of symmetry for the distribution of the normalized hoop stress.

In Fig. 6, the distribution of the normalized hoop stress σ_θ/σ at $\rho = 2$, $\theta = 0$ and π in the z -direction for $a/b = 2$ and different values of λ is presented. The distributions of the normalized hoop stress for $\lambda = -2$ and $\lambda = 2$ show an interesting mirror-reversed relation, which is not obvious from the material model (8.1). However, this property holds strictly and a proof for a particular case is given for illustration in “11”. It can be observed that the normalized hoop stress basically keeps constant along the thickness of the plate for $\lambda = 0$. The maximum value occurs at $z = -h/2$ for $\lambda = -2$, where the stiffness is the largest. Similarly, the maximum

Table 1 Elastic constants of Al_2O_3 (unit: GPa)

c_{11}^0	c_{12}^0	c_{13}^0	c_{33}^0	c_{55}^0
460.2	174.7	127.4	509.5	126.9

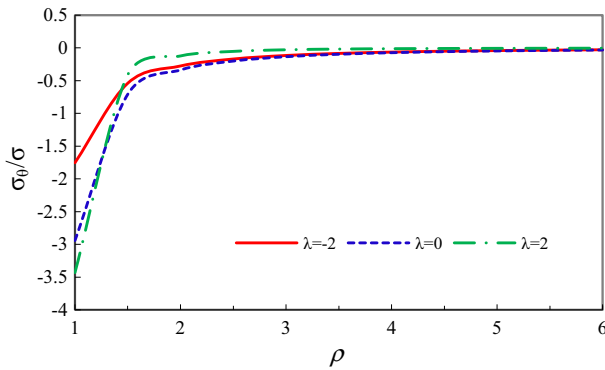


Fig. 4 Distribution of normalized hoop stress σ_θ/σ in the ρ -direction for $a/b = 2$ and different values of λ

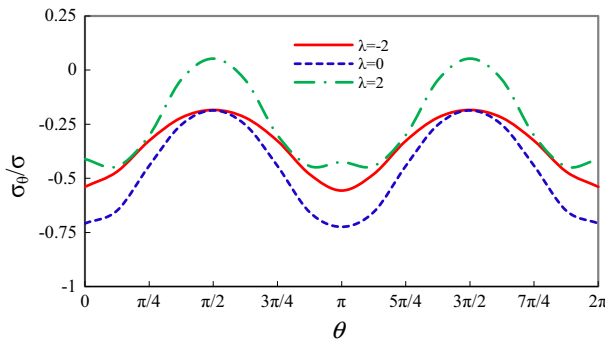


Fig. 5 Distribution of normalized hoop stress σ_θ/σ at $\rho = 1.5$ in the θ -direction for $a/b = 2$ and different values of λ

value occurs at $z = h/2$ for $\lambda = 2$. It is also noted that the normalized hoop stress values for $\theta = 0$ are the same as those for $\theta = \pi$ due to the symmetry of the problem.

In Fig. 7, the curves of the normalized hoop stress σ_θ/σ at $\rho = 1.5$ versus λ for different values of a/b are depicted. It is shown that the normalized hoop stress first slowly decreases and then rapidly increases with λ , and the turning point is in the vicinity of $\lambda = 1$. The larger the value of a/b , the more obvious the turning. The absolute value of the normalized hoop stress increases with a/b for certain λ .

Figure 8 shows the distribution of the normalized hoop stress σ_θ/σ in the z -direction for $\lambda = 0$, $a/b = 2$ and different values of ρ . In order to discuss the approximation caused by using Saint-Venant principle on the hole edge, a comparison is made between the 2D elasticity solution [1] and our 3D elasticity solution. It is

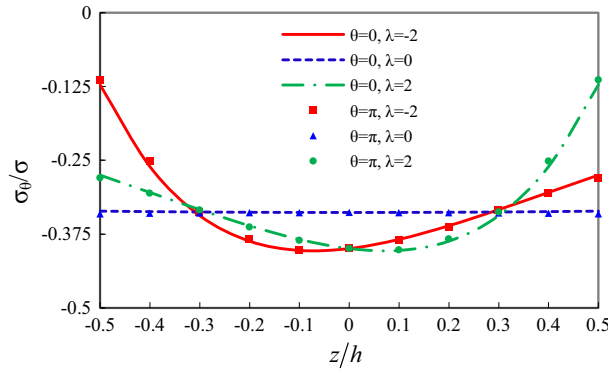


Fig. 6 Distribution of normalized hoop stress σ_θ/σ at $\rho = 2$, $\theta = 0$ and π in the z -direction for $a/b = 2$ and different values of λ

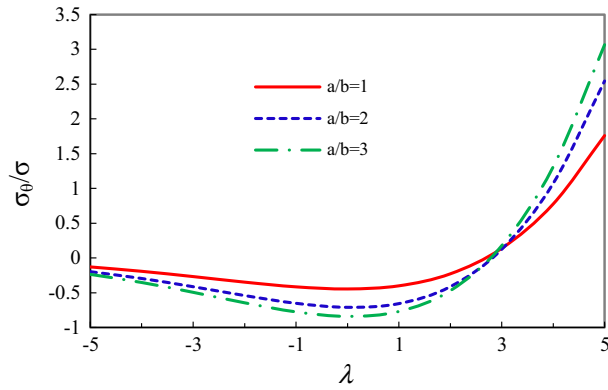


Fig. 7 Distribution of normalized hoop stress σ_θ/σ at $\rho = 1.5$ versus λ for different values of a/b

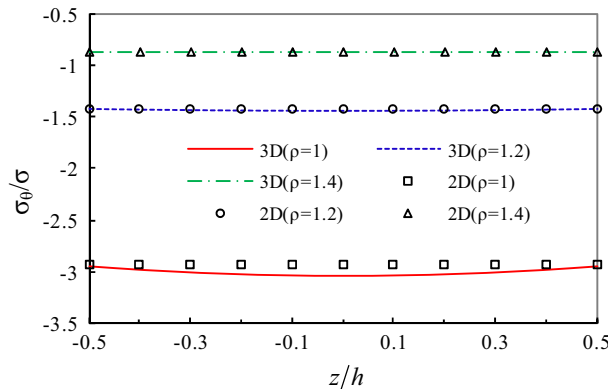


Fig. 8 Distribution of normalized hoop stress σ_θ/σ in the z -direction for $\lambda = 0$, $a/b = 2$ and different values of ρ

noted that the 2D elasticity solution is accurate enough because Saint-Venant principle is not employed and the uniform distribution of the 2D elasticity solution in the thickness of the plate can be established for the problem of an elliptical hole subject to a uniform pressure applied on the boundary. It is seen that there is a distinct difference between the 2D and 3D elasticity solutions on the edge of the hole. Outside the domain from the edge of the hole with the size of about the thickness of the plate, the present 3D elasticity solution agrees well with the 2D elasticity solution.

9 Conclusions

England–Spencer plate theory for a transversely isotropic functionally graded plate expresses the general solution of the governing equations in terms of four analytical functions. In an approximate sense, the boundary conditions can be expressed by four real functions, which correspond to the general solution. In this paper, we show that for the first kind basic problem, the boundary conditions can be rewritten as two complex function equations, thus eventually transforming the original problem into a complex function theory problem. This enables us to solve the equilibrium problems of FGM plates subject to different loads applied on the boundary of the plate by using the conformal mapping technology and the Cauchy integral method.

3D elasticity solutions are obtained for a transversely isotropic FGM plate containing an elliptical hole subject to loads at infinity or on the boundary of the hole. As for the case of loads applied at infinity, the analytical expressions and concentration factors of the resultant forces N_θ and M_θ for six typical cases are presented. It is found that the expression of the resultant force N_θ on the boundary of the elliptical hole in an FGM plate is exactly the same as that in a homogeneous plate and is also independent of the material constants and moments applied at infinity. When the elliptical hole degenerates to the circular one, the present elasticity solutions are consistent with those obtained in our previous work [21]. Numerical results are presented to consider an infinite FGM plate containing an elliptical hole subject to internal pressure applied uniformly on the hole boundary. It is shown that the gradient index and the shape of the hole have a serious impact on the stress field near the hole and little effect far away from the hole, where the stresses vanish at infinity.

It is strengthened that the obtained analytical solutions exactly satisfy the equilibrium equations of the plate and the traction boundary conditions on the upper and lower surfaces of the plate. Approximations are only made to satisfy the boundary conditions on the cylindrical edge of the plate. Outside the domain from the edge of the hole with the size of about the thickness of the plate, the present elasticity solutions are accurate enough to serve as a benchmark to check the validity and accuracy of any simplified plate theories or numerical methods when employed in the analysis of FGM plates.

Acknowledgments The work was supported by the National Natural Science Foundation of China (Nos. 11202188, 11272281 and 11321202), the Specialized Research Fund for the Doctoral Program of Higher Education (No. 20130101110120) and Program for Innovative Research Team of Zhejiang Sci-Tech University. The authors are also very grateful to the anonymous reviewers for their insightful comments and kind suggestions, which have greatly improved the quality of the manuscript.

11 Appendix

If there is no transverse load applied on the top and bottom of the plate, the expressions of the in-plane stresses in the plate are [19]:

$$\sigma_x + \sigma_y = \left(c_{11} + c_{12} - 2 \frac{c_{13}^2}{c_{33}} \right) \left\{ \frac{2}{\kappa_1 - 1} \left[\phi'(\zeta) + \overline{\phi'(\zeta)} \right] - 4 \left(z + \frac{\kappa_2}{\kappa_1} \right) \left[\beta'(\zeta) + \overline{\beta'(\zeta)} \right] \right\}. \quad (11.1)$$

$$\begin{aligned} \sigma_y - \sigma_x + 2i\sigma_{xy} = & 4c_{66} \left[\bar{\zeta} \phi''(\zeta) + \psi'(\zeta) \right] - \frac{16c_{66}}{\kappa_1 - 1} R_1 \phi'''(\zeta) \\ & + 8c_{66} \left(z + \frac{\kappa_2}{\kappa_1} \right) \bar{\zeta} \beta''(\zeta) + 8c_{66} z \alpha''(\zeta) \\ & - 32c_{66} \left(R_2 - \frac{\kappa_2}{\kappa_1} R_1 \right) \beta'''(\zeta). \end{aligned} \quad (11.2)$$

Without loss of generality, we consider for illustration an infinite plate with a circular hole. In this case, $m = 0$, and we have from Eq. (7.7) that

$$\{\gamma^1\} = \{0\}. \quad (11.3)$$

Substituting Eq. (11.3) into Eqs. (7.6) and (7.8) and noticing Eqs. (7.9), (5.19) and (5.20), we obtain

$$\begin{aligned} \phi(\eta) &= 0, \quad \beta(\eta) = 0, \\ \psi(\eta) &= \frac{2R}{\eta} \frac{b_7 N_n^b}{a_1 b_7 - 2a_6^2} = B_1(\eta) \frac{b_7 N_n^b}{a_1 b_7 - 2a_6^2}, \\ \alpha'(\eta) &= -\frac{2R}{\eta} \frac{a_6 N_n^b}{a_1 b_7 - 2a_6^2} = -B_1(\eta) \frac{a_6 N_n^b}{a_1 b_7 - 2a_6^2}, \end{aligned} \quad (11.4)$$

from which we can further derive

$$\begin{aligned} \phi(\zeta) &= 0, \quad \beta(\zeta) = 0, \\ \psi'(\zeta) &= B_2(\zeta) \frac{b_7 N_n^b}{a_1 b_7 - 2a_6^2}, \quad \alpha''(\zeta) = -B_2(\zeta) \frac{a_6 N_n^b}{a_1 b_7 - 2a_6^2}. \end{aligned} \quad (11.5)$$

Substituting Eqs. (8.1) and (11.5) into Eqs. (11.1) and (11.2) leads to

$$\sigma_x + \sigma_y = 0. \quad (11.6)$$

$$\sigma_y - \sigma_x + 2i\sigma_{xy} = 4N_n^b B_2(\zeta) c_{66}^0 e^{\lambda \left(\frac{z}{h} + 0.5\right)} \frac{b_7 - 2a_6 z}{a_1 b_7 - 2a_6^2}. \quad (11.7)$$

Substituting Eq. (8.1) into the expressions of constants a_1 , a_6 and b_7 defined in [19] gives rise to

$$\begin{aligned} a_1 &= 4 \int_{-h/2}^{h/2} c_{66}(z) dz = 4c_{66}^0 e^{0.5\lambda} \frac{h}{\lambda} (e^{0.5\lambda} - e^{-0.5\lambda}) \equiv 4c_{66}^0 e^{0.5\lambda} A_1(\lambda), \\ a_6 &= 4 \int_{-h/2}^{h/2} c_{66}(z) z dz = 4c_{66}^0 e^{0.5\lambda} \left[\frac{h^2}{2\lambda} (e^{0.5\lambda} + e^{-0.5\lambda}) - \frac{h^2}{\lambda^2} (e^{0.5\lambda} - e^{-0.5\lambda}) \right], \\ &\equiv 4c_{66}^0 e^{0.5\lambda} A_6(\lambda) \\ b_7 &= 8 \int_{-h/2}^{h/2} c_{66}(z) z^2 dz = 8c_{66}^0 e^{0.5\lambda} \left[\left(\frac{h^3}{4\lambda} + \frac{2h^3}{\lambda^3} \right) (e^{0.5\lambda} - e^{-0.5\lambda}) - \frac{h^3}{\lambda^2} (e^{0.5\lambda} + e^{-0.5\lambda}) \right]. \end{aligned} \quad (11.8)$$

As we can see, both $A_1(\lambda)$ and $B_7(\lambda)$ are even functions of λ , and $A_6(\lambda)$ is an odd function of λ . Making use of Eq. (11.8), we can obtain from Eq. (11.7) that

$$\sigma_y - \sigma_x + 2i\sigma_{xy} = e^{\lambda \frac{z}{h}} B_2(\zeta) N_n^b \frac{B_7(\lambda) - 2A_6(\lambda)z}{A_1(\lambda)B_7(\lambda) - 2A_6^2(\lambda)}. \quad (11.9)$$

Then, it is obvious that all the three in-plane stresses σ_x , σ_y and σ_{xy} (or σ_r , σ_θ and $\sigma_{r\theta}$) have the mirror-reversed relationship between the pairs (λ, z) and $(-\lambda, -z)$ when a uniform pressure N_n^b is applied on the edge of a circular hole. For the elliptical hole, the proof is similar, but more tedious, and it is left for the interested reader.

References

1. Muskhelishvili, N.I.: Some Basic Problems of the Mathematical Theory of Elasticity. Noordhoff, Netherlands (1953)
2. Savin, G.N.: Stress Distribution Around Hole. Pergamon Press, New York (1961)
3. Lekhnitskii, S.G.: Anisotropic Plate. Gordon and Breach, New York (1968)
4. Zhang, L.Q., Lu, A.Z., Yue, Z.Q., Yang, Z.F.: An efficient and accurate iterative stress solution for an infinite elastic plate around two elliptic holes, subjected to uniform loads on the hole boundaries and at infinity. Eur. J. Mech. A Solids **28**, 189–193 (2009)
5. Pan, Z.X., Cheng, Y.S., Liu, J.: Stress analysis of a finite plate with a rectangular hole subjected to uniaxial tension using modified stress functions. Int. J. Mech. Sci. **75**, 265–277 (2013)

6. Sharma, D.S.: Moment distribution around polygonal holes in infinite plate. *Int. J. Mech. Sci.* **78**, 177–182 (2014)
7. Zhang, X.Z., Kitipornchai, S., Liew, K.M., et al.: Thermal stresses around a circular hole in a functionally graded plate. *J. Therm. Stresses* **26**, 379–390 (2003)
8. Kubair, D.V., Bhanu-Chandar, B.: Stress concentration factor due to a circular hole in functionally graded panels under uniaxial tension. *Int. J. Mech. Sci.* **50**, 732–742 (2008)
9. Kubair, D.V.: Stress concentration factor in functionally graded plates with circular holes subjected to anti-plane shear loading. *J. Elast.* **114**, 179–196 (2014)
10. Yang, Q.Q., Gao, C.F., Chen, W.T.: Stress analysis of a functionally graded material plate with a circular hole. *Arch. Appl. Mech.* **80**, 895–907 (2010)
11. Yang, Q.Q., Gao, C.F., Chen, W.T.: Stress concentration in a finite functionally graded material plate. *Sci. China Phys. Mech. Astron.* **55**, 1263–1271 (2012)
12. Mohammadi, M., Dryden, J.R., Jiang, L.Y.: Stress concentration around a hole in a radially inhomogeneous plate. *Int. J. Solids Struct.* **48**, 483–491 (2011)
13. Ashrafi, H., Asemi, K., Shariyat, M.: A three-dimensional boundary element stress and bending analysis of transversely/longitudinally graded plates with circular cutouts under biaxial loading. *Eur. J. Mech. A Solids* **42**, 344–357 (2013)
14. Mian, M.A., Spencer, A.J.M.: Exact solutions for functionally graded and laminated elastic materials. *J. Mech. Phys. Solids* **46**, 2283–2295 (1998)
15. Yang, B., Ding, H.J., Chen, W.Q.: Elasticity solutions for a uniformly loaded rectangular plate of functionally graded materials with two opposite edges simply supported. *Acta Mech.* **207**, 245–258 (2009)
16. England, A.H., Spencer, A.J.M.: Complex variable solutions for inhomogeneous and laminated elastic plates. *Math. Mech. Solids* **10**, 503–539 (2005)
17. England, A.H.: Complex variable solutions for an inhomogeneous thick plate containing a hole or a crack. *Math. Mech. Solids* **9**, 445–471 (2004)
18. England, A.H.: Bending solution for inhomogeneous and laminated elastic plates. *J. Elast.* **82**, 129–173 (2006)
19. Yang, B., Ding, H.J., Chen, W.Q.: Elasticity solutions for functionally graded rectangular plates with two opposite edges simply supported. *Appl. Math. Model.* **36**, 488–503 (2012)
20. Yang, B., Chen, W.Q., Ding, H.J.: Elasticity solutions for functionally graded annular plates subject to biharmonic loads. *Arch. Appl. Mech.* **84**(1), 51–65 (2014)
21. Yang, B., Chen, W.Q., Ding, H.J.: 3D elasticity solutions for equilibrium problems of transversely isotropic FGM plates with holes. *Acta Mech.* **226**(5), 1571–1590 (2015)